MORP: Data-Driven Multi-Objective Route Planning and Optimization for Electric Vehicles

ANKUR SARKER, HAIYING SHEN, and JOHN A. STANKOVIC, University of Virginia, USA

The Wireless Power Transfer (WPT) system that enables in-motion charging (or wireless charging) for Electric Vehicles (EVs) has been introduced to resolve battery-related issues (such as long charging time, high cost, and short driving range) and increase the wide-acceptance of EVs. In spite of many previous works on ubiquitous data-driven traffic flow management for traditional vehicles, no research has been devoted to ubiquitous data-driven optimal route determination for EVs with WPT, where charging sections are installed in the road network to accommodate wireless charging. In this paper, we study the WPT system with the objectives of minimizing energy consumption, travel time, charging monetary cost on the way, and range anxiety for online EVs. Specifically, we propose the *Multi-Objective Route Planner* system (MORP) to guide EVs for the multi-objective routing. MORP incorporates two components: traffic state prediction and optimal route determination. For the traffic state prediction, we conducted analysis on a traffic dataset and observed spatial-temporal features of traffic patterns. Accordingly, we introduce the horizontal space-time Autoregressive Integrated Moving Average (ARIMA) model to predict vehicle counts (i.e., traffic volume) for locations with available historical traffic data. And, we use the spatial-temporal ordinary kriging method to predict vehicle counts for locations without historical traffic data. Based on vehicle counts, we use the non-parametric kernel regression method to predict velocity of road sections, which is used to predict travel time and then, energy consumption of a route of an EV with the help of the proposed energy consumption model. We also estimate charging monetary cost and EV related range anxiety based on unit energy cost, predicted travel time and energy consumption, and current onboard energy. We design four different cost functions (travel time, energy consumption, charging monetary cost, and range anxiety) of routing and formulate a multi-objective routing optimization problem. We use the predicted parameters as inputs of the optimization problem and find the optimal route using the adaptive epsilon constraint method. We evaluate our proposed MORP system in four different aspects (including traffic prediction, velocity prediction, energy consumption prediction, and EV routing). From the experimental studies, we find the effectiveness of the proposed MORP system in different aspects of the online EV routing system.

CCS Concepts: • **Information systems** → *Location based services*; • **Mathematics of computing** → Mathematical optimization; • **Human-centered computing** → Ubiquitous computing; • **Computer systems organization** → Embedded and cyber-physical systems;

Additional Key Words and Phrases: Wireless power transfer system, electric vehicle routing, multi-objective optimization, spatial-temporal traffic analysis

ACM Reference Format:
Ankur Sarker, Haiying Shen, and John A. Stankovic. 2017. MORP: Data-Driven Multi-Objective Route Planning and Optimization for Electric Vehicles. *Proc. ACM Interact. Mob. Wearable Ubiquitous Technol.* 0, 0, Article 0 (January 2017), 35 pages. https://doi.org/0000001.0000001

This research was supported in part by U.S. NSF grants ACI-1719397 and CNS-1733596, Microsoft Research Faculty Fellowship 8300751, and IBM PhD Fellowship.
Authors' address: Ankur Sarker; Haiying Shen; John A. Stankovic, University of Virginia, School of Engineering, Charlottesville, VA, 22903, USA.

2474-9567/2017/1-ART0 $15.00
https://doi.org/0000001.0000001

1 INTRODUCTION

Ubiquitous data-driven urban computing has focused much attention in recent years on the design and maintenance of a better smart city incorporated with intelligent transportation systems to promote better safety and to conform to the residents and commuters of the city [55, 57]. In the ubiquitous urban computing concept, every sensor, person, vehicle, building, and street in urban areas can be treated as sensing and computing units for serving the people and the city. Ubiquitous traffic planning in urban spaces requires much more attention to increase the efficiency of existing road infrastructures [57]. According to a recent study [2], commuters in the city of Los Angeles spent an average 104 hours a year in traffic during congested peak hours, which accounted for an average cost of $2,408 per commuter and $9.6 billion per the city as a whole from direct and indirect costs. Ubiquitous data-driven intelligent city-level traffic flow control and individual trip guidance would alleviate the issues inherent in city-level traffic congestion [22, 26, 50, 58]. Usually, traffic flow is spatio-temporal (space and time-related) and ubiquitous traffic flow data from different locations of the city can be represented as a city's vibes and can help to explain mobility patterns of people. Ubiquitous data-driven individual trip guidance to reduce either travel time or energy/fuel consumption has been thoroughly studied as a way either to ensure lower travel time or to reduce green-house gas effects [16, 21, 26, 50]. However, it is vitally important to consider both travel time and energy consumption as the first two factors in ubiquitous vehicle routing at the same time with city-level traffic flow as dynamic components.

In conjunction with improved urban traffic planning, the use of EVs further enhances the ubiquitous urban traffic system and ensures a more environmentally friendly smart city. The recent developments in Electric Vehicles (EVs) have great potential; although, the wide-acceptance of EVs still depends on tackling battery related issues (e.g., long charging times, high cost, short driving range, and heavy battery weight) that EVs encounter with the usage of onboard battery cells as the sole power source. In consequence, the EV commuters are constantly anxious about the driving range and always mindful of the availability (or lack) of charging facilities (i.e., range anxiety). To resolve this problem, the Wireless Power Transfer (WPT) system is designed to transmit power to the online EVs (with inductive charging capability) so that EVs can be charged on the way by the charging sections installed on top of the roads [34, 39]. As a result, the battery related anxiety issues can be mitigated. As reported in [33], any sort of charging infrastructure of EVs is capable of substantially reducing range anxiety of EVs. However, it is also reported that experienced EV drivers would still exhibit less range anxiety than inexperienced drivers in the presence of WPT systems and range anxiety would not be diminished overnight [23, 36]. In addition, frequent acceleration and deceleration because of traffic signs and traffic congestion would introduce additional energy consumption and increase the range anxiety. Thus, battery-related range anxiety should be considered as a third routing factor of online EVs. Charging monetary costs should be considered as a fourth important factor in the routing of online EVs. The price of power from the grid is also spatio-temporal and always fluctuates due to the fluctuations of power supplies and demands [4, 38]. Based on traffic flow, the amount of power taken from a particular location of WPT systems would be changed as well as charging cost.

As shown in Figure 1, we consider the scenario where online EVs run in a road network and receive drive-through electricity from charging sections. A road network consists of nodes and edges, where a node is a location and an edge is a road section connecting two locations. EVs can be charged from any of the three charging sections in the road network. A charging section has a certain length and the EV can be charged only when an EV is driving upon it. An EV needs to pay for the amount of received power from the grid [38]. In this paper, we focus on routing in highways with fixed charging sections

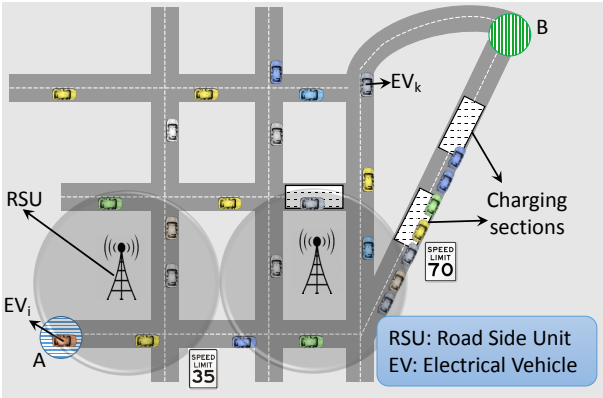

Fig. 1. Routing of online EVs.

and consider that our road network consists of mostly highways, although our approach can be directly applied to non-highways.

In a city or across-city area, suppose charging sections are deployed in certain locations in the highways [52]. Then, there arises a **problem:** *for a given EV driving from a source to a destination, how to choose a route so that i) the EV can successfully arrive at its destination with sufficient power supply on the way, and ii) the driver's range anxiety, charging monetary cost, travel time, and energy consumption can be minimized at the same time considering the current traffic flow?*

The solutions to this problem will contribute significantly to building intelligent transportation systems in urban computing. However, in spite of many previous works on ubiquitous data-driven route selection [6, 14, 19, 24, 32, 35, 40, 41, 43, 50, 56], there has been little research on this problem. The previous works are not for EVs with a WPT system and hence cannot be directly applied to meet the specific WPT-related requirements in such a scenario. In addition, these four factors are not positively related with each other and the consideration of these factors in ubiquitous data-driven vehicle routing problem is not trivial. For example, less travel time increases the energy consumption of vehicles. Range anxiety is dependent on the current onboard energy of EVs, total charging cost of EVs depends on traveling cost, and the location-based electricity price is determined by the power grid [38]. In addition, the impact of all four factors change based on spatio-temporal traffic flow in the road network. In this paper, we are motivated to fill in the gap in the literature by exploring a solution for the aforementioned ubiquitous data-driven vehicle routing problem.

In this paper, we propose a ubiquitous traffic data driven *Multi-Objective Route Planner* system (MORP) for online EVs that provides the optimal route for the aforementioned problem. MORP incorporates mainly two components: 1) *traffic state prediction* and 2) *optimal route determination.* First, we analyze the ubiquitous traffic flow data to realize the spatio-temporal traffic flow characteristics and devise the traffic state prediction approaches. We collected and analyzed 212 consecutive day-long historical hourly traffic flow data from 20 different highways and interstate roads in South Carolina (SC) from the Department of Transportation (DOT) website [1]. We made the following observations:

- specific time of the day affects the change of traffic flow (i.e., vehicle counts),
- in city level traffic flow, the free flow velocity is not necessarily observable at night,
- the velocity in a road section does not exhibit any obvious daily pattern over time and velocity distribution is usually skewed,

- the traffic counts in two time points (or two road sections) that are connected/next to each other are similar,
- regardless of the distance between two road locations, there is a correlation between the time of the day and the difference between the vehicle counts in the two road locations. It represents the pulse of the traffic flow.

Second, *traffic state prediction* helps to predict travel time and energy consumption of a route of an EV that are used later in the formulated optimization problem as inputs. If the predicted velocity of a road section is not accurate enough, it would affect the accuracy of the EV routing solution. Based on our data analysis observations, we build spatial-temporal regression models to predict the vehicle counts and velocity of each road section, which will be used to predict the travel time and energy consumption of a route of an EV in the optimization problem formulation. Some locations have historical traffic data while other locations do not have historical traffic data. For locations with historical traffic data, we introduce a horizontal space-time Autoregressive Integrated Moving Average (ARIMA) model based on observed temporal and spatial features of traffic to predict the vehicle counts at each hour. For locations without any historical traffic data, we apply spatial-temporal ordinary kriging method [13] and predict possible vehicle counts at each hour. Based on the predicted vehicle counts, we then use the non-parametric kernel regression model [20] to estimate velocity according to the correlation between vehicle counts and velocity. Eventually, we use the predicted velocity to estimate the travel time and energy consumption of a route of an EV, which are used in our formulated optimization problem. Third, in *optimal route determination*, we formulate a multi-objective optimization problem and find the optimal solution. We design four different objective functions for minimizing range anxiety, charging monetary cost, travel time, and energy consumption. For the power charging monetary cost, we consider that different sub-regions have different charging prices due to the variance of supply and demands of the power grid. We use the Polytomous Rasch model [18] as a scaling technique to represent the range anxiety of commuters. Then, we formulate a multi-objective optimization problem that ensures satisfying constraints of the state-of-charges (SOCs) (i.e., the percentage of energy stored in the battery) of EVs and the capacity of charging sections. To solve the multi-objective problem, we use adaptive epsilon constraint method [28], which is suitable for multiple objective functions and does not explicitly relax the constraints of the optimization problem.

We perform extensive simulation studies in Simulation for Urban MObility (SUMO) traffic simulator [25] based on real traffic data to evaluate the performances of our proposed MORP system in comparison with other route selection methods. The simulation results show that MORP outperforms other methods in terms of simultaneously minimizing range anxiety, charging monetary cost, travel time, and energy consumption. The simulation results also show that our proposed horizontal ARIMA model can more accurately make predictions than existing ARIMA model. We also show the simulation results on the traffic prediction using the ordinary kriging method, on the velocity prediction utilizing the non-parametric kernel regression, and on the energy consumption prediction based on our energy consumption model. We also evaluate the impact of traffic predictions on the performance of the route planning.

In summary, in this paper, we design and develop the MORP system, a data-driven multi-objective route planner for online EVs, which chooses the best available path for each EV in the road network considering the travel time, energy efficiency, charging cost, and range anxiety. Other factors can be easily incorporated into MORP for further consideration. The following are the major contributions of this paper:

- We analyzed a ubiquitous traffic dataset in terms of spatial-temporal features of traffic patterns, which serves as a foundation for building the prediction models for the traffic features (Section 3.2).

- Based on the dataset analytical observations, we introduce prediction models for the traffic features including traffic counts and velocity (Section 3.3).
- We develop an energy consumption model for EVs. We estimate travel time and energy consumption of a route of an EV based on the traffic prediction models in conjunction with the energy consumption model. Then, we use these estimations in the multi-objective optimization problem (Section 3.4).
- We design four different objective functions considering four factors (traveling time, energy consumption, charging cost, and range anxiety) and develop a multi-objective optimization problem. We find the solution to the proposed optimization problem using the adaptive epsilon constraint method (Section 3.5).
- We conduct extensive simulation studies based on real traffic data. The simulation results show the effectiveness of our MORP system in simultaneously achieving the multiple objectives and the effectiveness of the prediction models and energy consumption model (Section 4.2).

The rest of the paper is organized as follows. Section 2 presents the basic definitions and research problem of this paper. Then, Section 3 presents the system design of proposed multi-objective route planner. Section 4 evaluates the proposed route planner through extensive simulation studies. Section 5 discusses the existing literature. Finally, Section 6 concludes this paper with remarks on the future work.

2 BASIC CONCEPTS AND PROBLEM STATEMENT

In this section, we first introduce some basic definitions. Then, we briefly introduce our problem statement of finding a multi-objective routing of EVs.

Definition 2.1 (Road Network). A road network covers a large geographical-region and it consists of a finite set of locations $N = \{n_1, n_2, ..., n_t\}$ and a finite set of edges E where edge $e_{i,j}$ represents a road section connecting location n_i to location n_j.

Definition 2.2 (Road Section). Road section represents a small portion of the road network and it includes either single or multiple edges.

Definition 2.3 (State of Charge (SOC)). The SOC of an EV k represents the ratio between current stored energy in its battery pack and maximum energy capacity of the battery pack. Usually, SOC is in the certain range [0,1].

Definition 2.4 (Traffic Data Locations). In a dataset for a road network, traffic data locations are the set of locations $\{n_1, n_2, ..., n_i\}$ that have historical traffic data (average velocity, vehicle counts, etc.).

Definition 2.5 (Traffic State). For a road network, the traffic state or traffic scenario indicates the traffic flow (i.e., vehicle counts and average velocity) of its road sections at a particular time. Actually, average hourly velocity changes based on the traffic state. And, *travel time*, *energy consumption*, *charging monetary cost*, and *range anxiety* are dependent on the average hourly velocity. Thus, it is important to accurately predict the traffic states ahead such that an optimization algorithm can determine the most appropriate route. In this paper, we alternately use either "traffic state" or "traffic scenario".

Definition 2.6 (Travel Time). For a source to destination routing, the travel time means the required time to finish the trip based on the corresponding traffic scenario (e.g., average velocity).

Definition 2.7 (Energy Consumption). For a source to destination routing, the energy (or fuel) consumption signifies the required energy to finish the trip based on the corresponding traffic scenario (e.g., average velocity).

Table 1. Symbols and Definitions.

Notation	Definition
K	Total number of EVs
M	Total number of charging sections
s_i	The source of EV i
d_i	The destination of EV i
n_i	The location i in the region
$e_{i,j}$	The edge connecting locations n_i and n_j
$y_i(t)$	SOC of EV i at time t
cap_m	Total capacity of charging section m
$p_{\text{th},k}$	Lower value of SOC

Definition 2.8 (Range Anxiety). For the commuters of an EV, range anxiety represents the fear of fully depleting the onboard battery before reaching the destination. Based on the current traffic scenario, range anxiety mostly depends on current onboard energy and required energy to finish the trip (e.g., average velocity). The Consideration of range anxiety in EV route planning is important for better traveling experiences and it is reported that range anxiety would not be diminished overnight [23, 36].

Definition 2.9 (Charging Monetary Cost). Charging monetary cost refers to the money required to get the energy from charging sections of the WPT system, which fluctuates due to the regional supplies and demands of the power grid [4, 38]. In addition, for a given traffic scenario (e.g., average velocity), the charging monetary cost also depends on the amount of energy an EV can get from the WPT. Thus, it is possible to choose some charging sections over others which require a lower monetary cost. Here, we consider the fixed placements of charging sections.

Definition 2.10 (EV Routing Problem). For an EV k, routing problem is a path finding problem which seeks a feasible path τ^k from source location to destination location.

Suppose there are K number of online EVs running on the different road sections of a region, and each of them has a certain SOC and a source-destination pair. Here, SOC must be in a certain range (0.25–1) for the sake of battery health. Let $p_{\text{th},k}$ be the lower limit of SOC for EV k to maintain healthy battery state and the continuous vehicle operation. Also, there are M number of charging sections installed on the different edges of the region and cap_m is the capacity of charging section m. Table 1 shows the parameters related with basic definitions. EVs can receive energy from the charging sections if the charging sections are on and they drive on top of the charging sections. We assume the charging sections are always on for the sake of simplicity. The motivation of this work is to plan and distribute the real-time routing of the EVs so that EVs can reach their destinations satisfying their onboard energy constraint, lower travel time, lower chagrining cost, and lower range anxiety. However, EVs share the road with other vehicles and it is necessary to predict the future traffic state of the road network. Traffic scenario prediction requires the construction of prediction models based on the analysis of the historical traffic data in the region. Thus, the first problem is *how to predict the future traffic congestions, traveling time, and energy requirements of different road sections based on available historical traffic data?* After predicting the travel time and energy consumption of different road sections, we can determine the optimal routes for the EVs on different road sections considering their SOCs, charging section placements, charging cost, traveling time, and range anxiety (which is related to current SOC). Different EVs may have different amounts of onboard energy and they may need different amounts of required energy. Thus, it is desirable to finish their trips while satisfying their energy, travel time, charging monetary cost, and range anxiety constraints. Thus, the second problem is to *reroute the EVs so that EVs can satisfy the available energy constraints, minimize four costs (energy consumption, traveling time, charging monetary cost, and range anxiety), and finish their trips.*

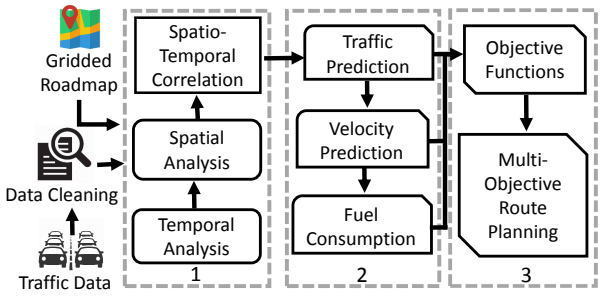

Fig. 2. The framework of MORP.

In next section, we present the system design of the proposed MORP system to distribute the EVs among different edges of the region.

3 SYSTEM DESIGN

In this section, at first, we present the framework of the proposed MORP system (Section 3.1). Then, we discuss our observations from the ubiquitous traffic data (Section 3.2). Next, we present the available traffic, velocity, and energy consumption predictions based on the traffic data analysis (in Section 3.3 and Section 3.4, respectively). Finally, we present the multi-objective optimization problem and an approach to find its solution (Section 3.5).

3.1 Framework of MORP

In the MORP system, ubiquitous traffic flow data is collected to the cloud (or fog [46]) periodically. Then, the cloud (or fog) processes the collected data for traffic state prediction and then solves the optimization problem and finds the optimal route for each EV. Finally, the cloud (or fog) sends the optimal route to each EV. To develop the MORP system, our work consists of the following three stages as shown in the three dashed boxes in Figure 2.

Traffic data analysis. We analyze the spatial-temporal traffic correlation for different road sections and try to determine some patterns (if any) with respect to (*w.r.t.*) time and space which are used in traffic state prediction later.

Traffic state prediction. The cloud (or fog) needs to predict vehicle counts, velocity, and energy consumption of a route of an EV. Based on the vehicle density and traffic flow rate, the energy consumption and travel time of a route change. In addition, range anxiety and charging monetary cost depend on traffic flow rate indirectly. Thus, it is very crucial to accurately predict vehicle counts so that route planning is accurate and can satisfy future traffic flow. Here, we use ARIMA and ordinary kriging to predict the vehicle counts from which we predict the average velocity using non-parametric kernel regression. We then use average velocity in our proposed energy consumption model to predict the energy consumption and also predict travel time for a route of an EV.

Multi-objective route planning. We design four different objective (goal) functions: energy consumption, travel time, charging monetary cost, and range anxiety. The energy consumption and travel time of a given route are calculated based on the predicted vehicle counts and velocity of the same route. Charging monetary cost is also determined based on predicted velocity and unit energy price. Range anxiety is indirectly dependent on predicted velocity. At first, we calculate the values for four different objective functions. Then, we formulate the optimization problem to achieve these objective functions and use the adaptive epsilon constraint method to find the solution (e.g., an optimized route satisfying these objective functions).

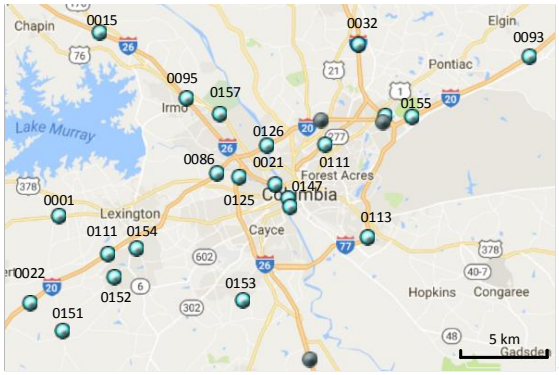

Fig. 3. Map of the road network (with the traffic data locations).

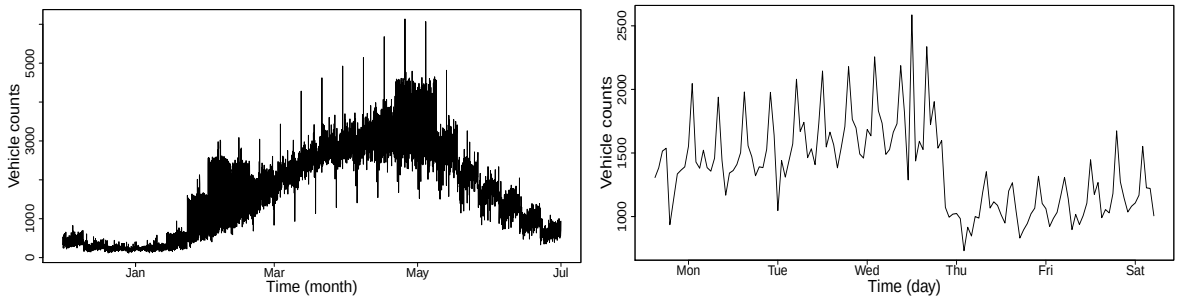

(a) 212 consecutive day-long

(b) 7 consecutive day-long

Fig. 4. Vehicle counts from one traffic location.

In the following section, we present traffic data analysis, traffic state prediction, and multi-objective route planning, respectively.

3.2 Data Analysis of Different Road Sections

We collected 212 consecutive day-long historical hourly traffic flow data (December 1, 2016 – June 30, 2017) from the SC DOT website for 20 locations in 3 interstate routes, 9 US routes, and 6 state routes as shown in Figure 3. The scaling of the map is 30 km×20 km. The cyan dots represent different locations in highways for collecting traffic data. For each data location, SC DOT collects hourly eastbound/westbound vehicle counts, average hourly velocity of these vehicles, and average hourly vehicle counts of the last three months. We collected the data manually and used the R programming language to analyze the data. It is known that traffic flow data is spatial-temporal in nature. That is, the traffic scenario (e.g., vehicle counts and velocity) at a location may exhibit a certain pattern over time, and the traffic scenario at neighboring locations at times may exhibit a certain correlation. We analyze the dataset to study the spatial-temporal features. In the following, we only show the significant spatial-temporal features discovered from the data analysis.

Temporal analysis. At first, we study the temporal correlations between vehicle counts and time of the day of different locations. More specifically, we try to answer the following questions:

Q1. For a given location, does the vehicle counts exhibit a certain pattern over time? Figure 4(a) shows hourly (eastbound) vehicle counts of 212 consecutive days from a randomly chosen location (id 0086). We can see that the daily vehicle counts gradually changes over time. More exactly, from December to January vehicle counts increase gradually, from February to May vehicle counts are more stable, and

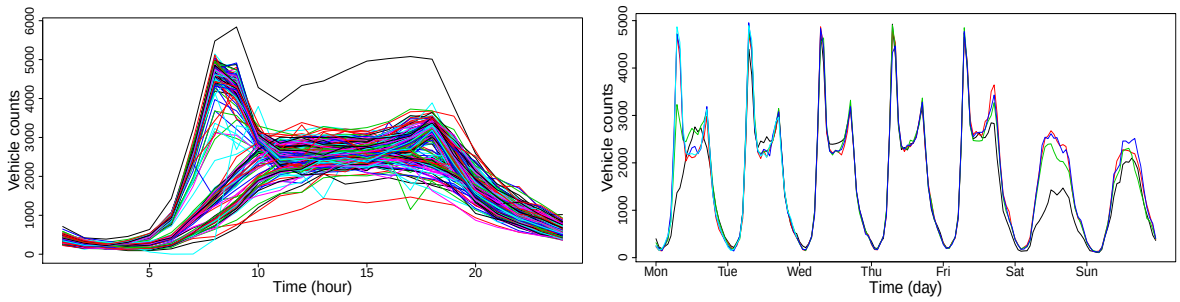

(a) Hourly vehicle counts

(b) Daily vehicle counts

Fig. 5. Vehicle counts analysis.

from May to June vehicle counts decrease. In addition, there are peaks of vehicle counts on Tuesday, Wednesday, and Thursday. Vehicle counts are also peaked based on the popular public holidays; e.g., vehicle counts are higher than usual on February 14 (Valentine's Day) and May 14 (Mother's Day). Then, we zoom-in the data from the same location and check vehicle counts for a randomly selected week (January 2 to January 8). Figure 4(b) shows the vehicle counts for 7 days (Monday – Sunday). We can see that the distribution of the vehicle counts is not uniform throughout the day and there are similar patterns on weekdays and/or weekends. We also find that the horizontal deviation of vehicle counts is smaller than the vertical deviation of vehicle counts.

Next, we closely study the correlations between vehicle counts and time. Figure 5(a) shows hourly 212 consecutive day-long vehicle counts for the same location, where each line represents vehicle counts for a day and there are 212 lines in total. We see that the vehicle counts for different days exhibit similar hourly patterns. More clearly, there is a sudden rise in vehicles counts around 6 am and it reaches a stable state around 10 am. There are also two separate trends for two groups of days: weekdays and weekends. Weekdays' vehicle counts are very close to each other and weekends' vehicle counts are more diverse. Figure 5(b) shows the hourly vehicle counts per week for five weeks (January 30 to 5 March) for the same location. As we have already discussed, the vehicle counts of these five weeks are comparable and vehicle counts of different weeks also show similar daily patterns. Particularly, we find that weekdays' traffic easily resembles one pattern and weekends' traffic resembles another pattern. We conducted the same analysis on all other locations and observed similar phenomena. Based on an analysis of the above findings, we can make the following observation:

Observation 1. The vehicle counts exhibit a certain pattern over time and horizontal deviation of vehicle counts are smaller than the vertical deviation of vehicle counts. To predict the vehicle counts at a specific time t of a day, we would utilize the vehicle counts at that time, t of previous days.

Q2. For a given location, does the average hourly velocity exhibit a certain pattern over time? Then, we analyze the hourly average velocity for all 20 locations and they show similar phenomena. Figure 6(a) shows hourly average velocity for each day of the same randomly chosen location. Here, we remove the extreme outliers to more clearly show the results. The hourly average velocity does not resemble a specific pattern. Generally, if the speed limit of the roads is 65 mph, then the average velocity falls into the range of [60 mph,70 mph]. Figure 6(b) shows the average velocity in a week for five weeks (January 30 to March 5) for the same randomly chosen location. Then, we analyze average velocity distributions of different traffic locations and we find that the distributions are always skewed as shown in Figure 7(a) where different lines represent the data from different traffic locations. In addition, we analyze the average velocity distribution of two weeks (January 9 to January 23) from another randomly chosen location

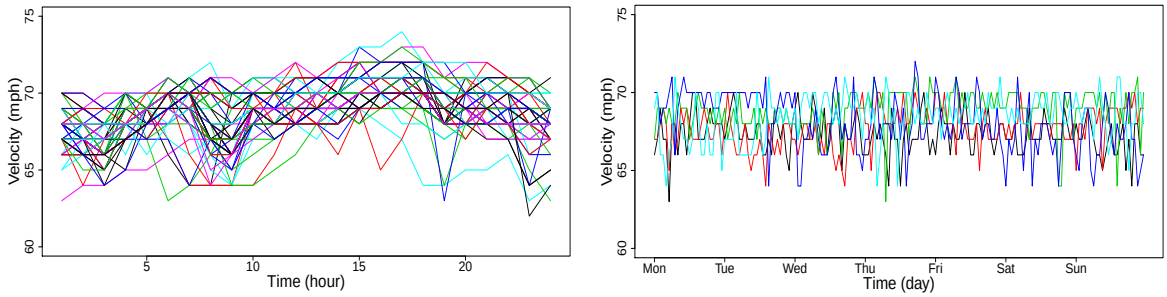

(a) Hourly average velocity (b) Daily average velocity

Fig. 6. Average velocity analysis.

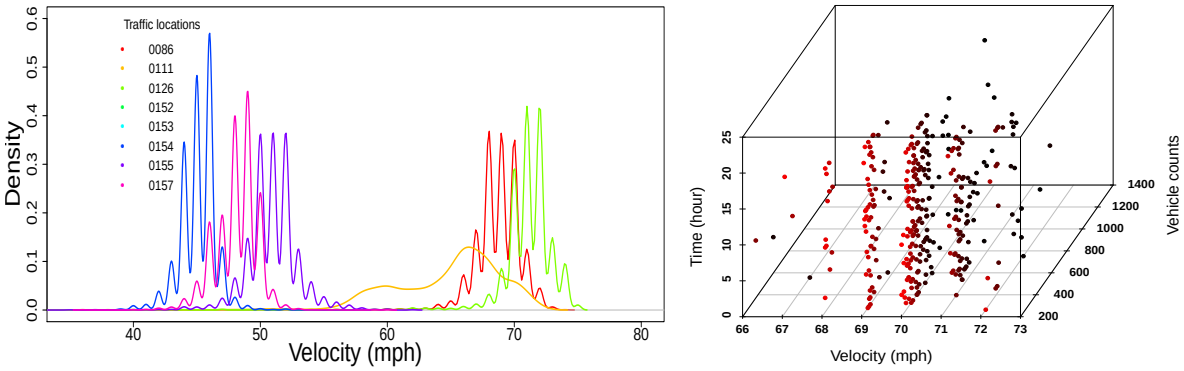

(a) Average velocity distribution (b) Average velocity, vehicle counts, and time

Fig. 7. Distributions of average velocity.

(id 0126) *w.r.t.* time and vehicle count as shown in Figure 7(b). We find that there are three bands of velocity points *w.r.t.*the speed limit of the road section. Sometimes, the vehicle counts and average velocity are lower than usual due to the arrival rate of vehicles. From the above analysis, we can make the following observation:

Observation 2. The average velocity does not exhibit a certain pattern over time and distributions of the velocity are skewed. Fortunately, we can predict average velocity at a road section based on the vehicle counts of the road section using nonparametric prediction methods as in previous work [48].

Spatial analysis. We seek the following spatial relationship *w.r.t.* the correlations of vehicle counts and hourly average velocity from different locations.

Q1. Can we predict the near-future traffic flow (i.e., vehicle counts or average velocity) at a location using the current traffic flow of its preceding locations?

Figure 8(a) shows the scatter plot of 212 consecutive day-long vehicle counts from two randomly chosen neighboring data locations (id 0086 and 0126) with 1 hour time lag (as collected data is hourly accumulated). That is, if location n_i is preceding to location n_{i+1} in traffic flow, the vehicle counts of location n_i at hour $t-1$ (x) and the vehicle counts of location n_{i+1} at hour t (y) produces a point (x, y) in the figure. From the figure, we can see that first vehicle counts and second vehicle counts show significant positive correlations which means if one vehicle count changes, other vehicle counts also change in the same direction. Also, we conduct the Pearson correlation coefficient test by applying two vehicle counts

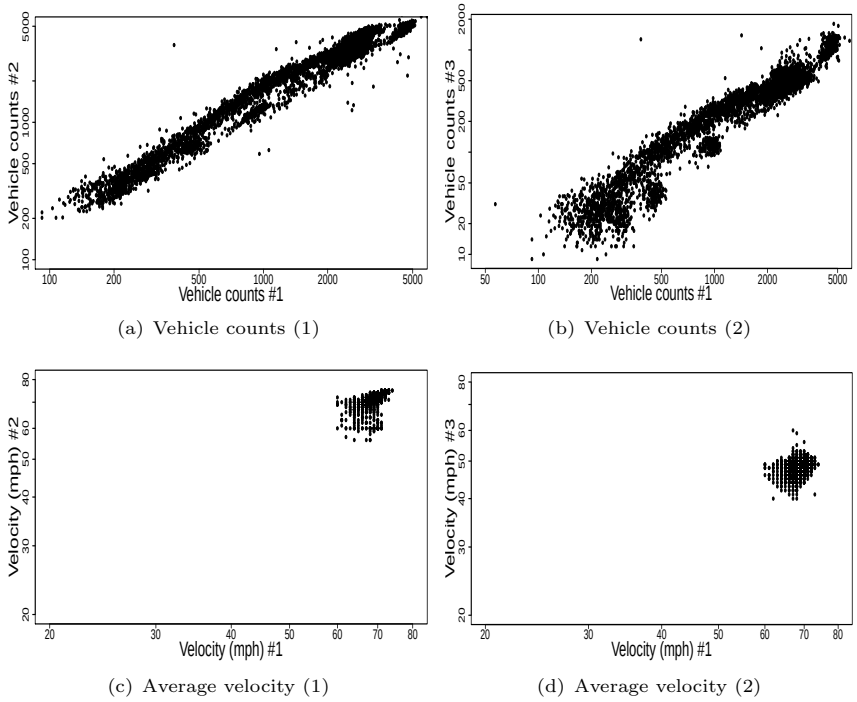

(a) Vehicle counts (1) (b) Vehicle counts (2)

(c) Average velocity (1) (d) Average velocity (2)

Fig. 8. Correlations among different traffic locations.

into the correlation function [29]. If population correlation coefficient is closer to 1 and p-value of the test is less than 0.5, then it means two variables are strongly correlated more than 95% of the time. In our case, the population correlation coefficient equals 0.96 and p-value of the test is less than 2.2×10^{-16}. Thus, two vehicle counts are significantly correlated in more than 95% of the test cases. Figure 8(b) shows the scatter plot of 212 consecutive day-long vehicle counts from another pair of randomly chosen neighboring data locations (id 0086 and 0157) with 1 hour time lag and we can conclude the same observation.

Then, we analyze the correlation between two average velocity values (with 1 hour time lag) for the first pair of randomly chosen neighboring traffic data locations as in Figure 8(a). Figure 8(c) shows the scatter plot of 212 day-long average velocity values for the two different traffic data locations and we can see that the two different velocities from two different locations are overlapped with each other. Figure 8(d) shows the scatter plot of 212 day-long average velocity values for the second pair of two different traffic data locations as in Figure 8(b). Thus, we can conclude the following observation:

Observation 3. Vehicle counts exhibit spatial correlations among different traffic locations. Thus, we can utilize neighbors' vehicle counts for traffic flow predictions.

Finally, we analyze the hourly change rate of vehicle counts among different locations using all collected traffic data. We grouped all data locations using the intermediate distance between any two locations is less than 16.75 km, and obtained three specific groups. There are eight (0086, 0111, 0126, 0152, 0153, 0154, 0155, and 0157), eight (0001, 0022, 0111, 0151, 0152, 0153, 0154, and 0113)), and seven (0015, 0021, 0032, 0093, 0095, 0147, and 0086) data locations in each group, respectively. Figure 9 shows the change rate of vehicle counts of each location in a group (consists of eight data locations). Five out of the eight locations are neighbors. We calculated change rate as follows: 100×(current hour's vehicle counts - previous hour's vehicle counts)/previous hours' vehicle counts. Specifically, Figure 9(a) shows the hourly

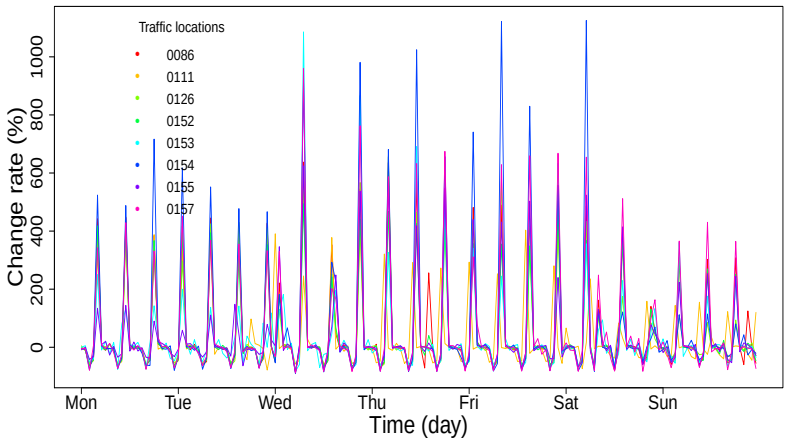

(a) Week 1

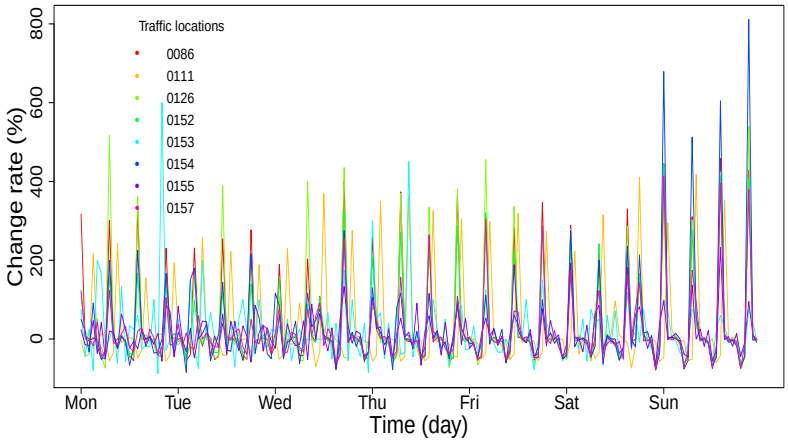

(b) Week 2

Fig. 9. The change rate of neighboring traffic data locations.

change rate in the one week (9 January to 15 January) and Figure 9(b) shows the hourly change rate in another week (2 January to 8 January). In the figure, each curve represents a seven-day long hourly change rate in a data location. We can see that there are clear daily patterns as the vehicle counts are stable and there is no obvious pattern for the first few days (Monday to Wednesday) of the week as it is the week just after the New Year holiday and vehicle counts are being stable over time. We find that the average vehicle counts on these days are lower than the average vehicle counts of the same days of the last three months. However, most of the change rates of vehicle counts are peaked at the same time. We also perform the same study for the other two groups and get similar results (figures are not shown here due to the space limit). Based on the above discussion, we can make the following observation:

Observation 4. The vehicle counts in close locations exhibit certain correlations.

Next, we present the traffic prediction procedures based on the spatial-temporal data analysis observations presented above.

3.3 Traffic Prediction of Different Road Sections

Here, we use ubiquitous traffic flow data to predict future vehicle counts. As mentioned in Section 3.1, it is very important to accurately predict future vehicle counts so that route planning is accurate *w.r.t.* four different objective functions. In our dataset, SC DOT only collected traffic data for certain locations and many locations do not have any traffic flow data. Indeed, in practice, it is likely that some locations do not have historical traffic data because of the reasons such as lacking sensing devices or data transmission failure. Therefore, we conduct two types of predictions: i) we predict the vehicle count values at locations with available traffic flow data, and ii) we predict the vehicles count values at locations without any historical traffic flow data.

3.3.1 Prediction for locations with historical data. We propose an ARIMA model to predict vehicle counts for locations with historical data. Usually, a space-time ARIMA model has two components: autoregression (AR) and moving average (MA). The AR component uses the dependent relationship between an observation and some number of lagged observations. The MA component uses the dependency between an observation and a residual error from a moving average in terms of the lagged observations. Based on the *Observation 1* and *Observation 3* from the spatial-temporal analysis in Section 3.2, we introduce the horizontal ARIMA model [44]. First, to predict vehicle counts in location n_i at time t_i, we use the historical vehicle counts at location n_i at time t_i on the previous days and the vehicle counts at location n_i until a certain time period before time t_i on the current day (*Observations 1*). In this way, the ARIMA model needs to consider the small moving average order. Second, we consider neighbor correlation or weight matrix of vehicle counts in neighboring locations. The proposed horizontal ARIMA model is relatively simple: it utilizes the time series of vehicle counts, and it does not try to forecast the cycles.

An existing work [11] considers average velocity as the scale factor of space-time ARIMA model to calculate the neighbor weight matrix. However, based on the spatial analysis in Section 3.2 (*Observation 2* and *Observation 3*), we consider vehicle counts as the scale factor. More specifically, we consider the neighbor weight matrix, W^l, a square $m \times m$ l^{th} order weight matrix. In the matrix element, $w_{i,j}^{(l)}$ represents the correlation of adjacent locations n_i and n_j with l^{th} temporal lag in terms of vehicle counts x_i and x_j. Dynamic spatial weight between two locations, $w_{i,j}^l(t)$, is calculated as a function of their relative vehicle counts (i.e., difference between $x_i(t)$ and $x_j(t)$ at a particular time t). If we see a drop of vehicle counts in one location, we expect this decreases vehicle counts in an adjacent location and vice versa.

For all location pairs (x_i, x_j) with spatial lag l, if location x_j is upstream of location x_i, the corresponding $w_{i,j}^l$ is calculated as follows:

$$w_{i,j}^l(t) = \frac{x_j(t) - x_i(t)}{x_i(t)}, \tag{1}$$

otherwise,

$$w_{i,j}^l(t) = \frac{x_i(t) - x_j(t)}{x_j(t)}. \tag{2}$$

The neighbor weight matrix tends to equilibrate the differentials of vehicle counts over space. Here, we can easily incorporate velocity as a scale factor of neighbor weight matrix in our system if necessary.

Finally, we can present the horizontal ARIMA model as follows. In our ARIMA model, there are horizontal autoregression and moving average terms with certain temporal lag. Also, there are adjacent locations' autoregression and moving average terms with single temporal lag. Here, we only consider

single temporal lag as we use hourly historical traffic data and vehicles can traverse from one location to another location in the road network within an hour based on their average velocities. Let $X(t)$ be an N-dimensional column vector containing the observations $x_i(t)$ (vehicle counts) on the location n_i, where $i = 1, 2, ..., V$, during each time interval t. Accordingly, the proposed horizontal ARIMA model can be described as follows:

$$\bar{x}(t) = \sum_{d=1}^{p} \theta_d x_{t-d*24} - \sum_{d=1}^{q} \psi_d \varepsilon_{t-d*24} + \sum_{l=1}^{V} \Theta_l W^l x_{t-1} - \sum_{l=1}^{V} \Psi_l W^l \varepsilon_{t-1} + \varepsilon_t, \tag{3}$$

where $\theta_{d,l}$ and $\psi_{d,l}$ are autoregressive and moving average parameters at temporal lag d and special lag l; p is the autoregressive order; q is the moving average order; ε_t is the white noise; Θ and Ψ are autoregressive and moving average parameters for adjacent locations, respectively; x_{t-d*24} and ε_{t-d*24} are autoregression and moving average terms of horizontal vehicle counts, respectively, with temporal lag $d*24$; and x_{t-1} and ε_{t-1} are autoregression and moving average terms of adjacent locations' vehicle counts with temporal lag 1, respectively. Thus, from Equation (3), we can state that the proposed ARIMA model considers the horizontal temporal lag and most recent observations in neighboring locations. Proposed ARIMA model produces forecasts based on prior values in the time series (AR terms) and the errors made by previous predictions (MA terms). This typically allows the model to rapidly adjust for sudden changes in trend (i.e., weather effects), resulting in more accurate forecasts.

Parameters Estimation. For our proposed horizontal ARIMA model, we need to estimate in total $(p + q + 2N)$ parameters. At first, we estimate the values of autoregressive order p and moving average order q using space-time autocovariance function. Then, we can use the maximum likelihood estimation method to estimate all other parameters (discussed in Appendix A).

3.3.2 Prediction for locations without historical data. If a traffic location (without any historical data) has a single incoming (or upstream) road section, we can use the prediction of vehicle counts of its preceding location (with historical traffic data) to approximately estimate the vehicle counts of this location (*Observation 4* in Section 3.2). However, this approach cannot be applied to a location with more than one incoming road section. To handle this case, we use the spatio-temporal ordinary kriging approach [47]. The basic idea of kriging is to predict the value of a function at a given location by computing a weighted average of the known values of the function in the neighborhood of the location. For a given location n_i, time t_i and vehicle counts x_i can be expressed as:

$$Z(x_i, t_i) = \mu + \varepsilon(x_i, t_i), \tag{4}$$

where μ is the original mean of the vehicle counts of all locations and $\varepsilon(x_i, t_i)$ is the random quality with mean zero. We use h to represent both the direction and distance *w.r.t.* to location n_i and use u to represent the time *w.r.t.* the original time t_i. Based on the nature of traffic flow, we can consider that the traffic flow data is intrinsic stationary (vehicle counts and average velocity of nearby locations are almost the same) and the variogram can be derived as follows:

$$\gamma(h, u) = \frac{1}{2V(h, u)} \sum_{2V(h,u)} \{[Z(x_i, t_i) - Z(x_i, t_i)]\}^2. \tag{5}$$

Thus, for a location o without historical traffic data, we can apply the spatio-temporal ordinary-kriging approach as follows:

$$\bar{Z}(x_o, t_o) = \sum_{i=1}^{V} \sum_{t_i=1}^{24} \lambda_{i,t_i} Z(x_i, t_i), \tag{6}$$

Table 2. Symbols and Definitions used in the traffic predictions.

Notation	Definition
W	Neighbor matrix
l	Temporal lag
$x_i(t)$	Traffic count of location i at time t
p	Autoregressive order
q	Moving average order
ε_t	White noise
Θ	Autoregressive parameters
Ψ	Moving average parameters
Z	Traffic data distribution
μ	Original average of vehicle counts
x	Vehicle counts
Ψ	Moving average parameters
α	Largance multiplier

where $\lambda_{i,t_i}, i = 1, 2, ..., V$, are the weights chosen to minimize the prediction error variance by the solution of the following functions:

$$\sum_{i=1}^{V}\sum_{t=1}^{24}\lambda_{i,t_i}\gamma[(x_i,t_i)-(x_j,t_j)]+\alpha(x_o,t_o)=\gamma[(x_j,t_j)-(x_o,t_o)], \tag{7}$$

where $\sum_{i=1}^{N}\sum_{t=1}^{24}\lambda_{i,t_i}=1$, $\gamma[(x_i,t_i)-(x_j,t_j)]$ is the semivariance between locations n_i and n_j at time t, and $\alpha(x_o,t_o)$ is the Lagrange multiplier introduced to minimize the error variance. Thus, from historic traffic data, we can get the optimal value of λ_{i,t_i} for each location n_i at time t based on Equation (7). Thus, we can easily predict the traffic data for another location $(x+h,u)$. Table 2 shows the parameters related to the traffic predictions.

So far, we have introduced how to predict the vehicle counts of a location using historical traffic data. In the next section, we present how to predict the average velocity based on the predicted vehicle counts, and then how to use the predicted velocity to predict the travel time and energy consumption for a route of an EV.

3.4 Prediction of Velocity, Travel Time, and Energy Consumption

We can predict the average velocity of each road section based on the predicted vehicle counts. We basically use the vehicle counts to figure out the expected velocity profile of each road section of the road network. Then, we can predict approximate travel time and energy requirements of each road section of the road network using the predicted velocity profile. Eventually, we can estimate the travel time and energy consumption of a route of an EV.

Based on the temporal analysis (*Observation 1* and *Observation 2*) in Section 3.2, we can consider speed limit as free-flow velocity of a road section. The (positive or negative) deviation from free-flow velocity of a road section causes a range of velocities of that road section. The vehicle counts can be used to estimate the deviation from free-flow velocity (*Observation 2*). First, we consider the following relationship among free-flow velocity, average velocity, and vehicle counts:

$$\bar{v}(x)=v_{free}+f_v(x), \tag{8}$$

where x is the vehicle counts, $\bar{v}(x)$ is the average velocity of vehicles, v_{free} is the free-flow velocity, and function $f_v(x)$ represents the velocity deviation function based on the total vehicle counts x. Next, we consider the non-parametric kernel regression [20] to predict velocity deviation based on the number of vehicles, $f_v(x)$ (*Observation 2*). Here, kernel regression is used to find a non-linear relation among

vehicle counts and velocity deviation. Kernel regression basically estimates the conditional expectation of a random variable. Then, we can write the above term $f_v(x)$ as follows:

$$f_v(x) = \frac{\sum_{i=1}^{v} K\left(\frac{x-x_i}{h}\right)\Delta v_i}{\sum_{i=1}^{v} K\left(\frac{x-x_i}{h}\right)}, \tag{9}$$

where v is the total number of observations of vehicle counts, $K_x(\cdot)$ and $K_t(\cdot)$ are the kernel functions, set to the Gaussian function based on its smoothness [31], x_i is the number of vehicles, Δv_i is velocity deviation from observation i, and h is the smoothing parameter influencing the estimation accuracy of regression which is determined according to the mean integrated squared error criterion [45]. Finally, we can predict the hourly average velocity $\bar{v}(x)$ based on $f_v(x)$ and Equation (8).

Now, based on the vehicle counts and three velocity values (speed limit, upper and lower ranges of velocities), we consider three different velocity profiles for a given edge in the road network (free flow velocity and positively and negatively deviated velocities from free flow velocity). Here, we further use truncated regression to consider a certain range of velocities [30]. In the case of truncated regression, we use two ranges of average velocity observations as the outcome variables in two cases, respectively and systematically exclude other velocities. Thus, the predicted average velocity at a specific time may cause less energy consumption or worse energy consumption based on different cases (e.g., velocity profiles).

Next, we design a power consumption model *w.r.t.* different applied forces in EV when it is crossing a road section with an average velocity. The EV's power consumption depends on different factors of the road sections. Let $y_k(t)$ represent the SOC of EV k at time t, and let $y(t) = [y_1(t)y_2(t)...y_m(t)]^\top$. Then, $y_k(t_k^e)$ and $y_k(t_k^l)$ represent the SOC of vehicle k when it enters and leaves a road section, respectively. From previous work [37], we can derive the amount of power required to move the EV k for a unit time period, denoted by $P_{\text{trac},k}$. However, it does not consider the force of rolling resistance and ignores battery energy transforming efficiency η_1 and powertrain working efficiency η_2. To additionally consider these factors, we calculate the amount of power required to move EV k for a unit time period as follows:

$$P_{\text{trac},k} = \frac{M_k a_k v_k + \frac{1}{2}\rho_{\text{air},k} C_{\text{d},k} {v_k}^3 + M_k g C_{\text{rr}} v_k}{\eta_1 \eta_2}, \tag{10}$$

where M_k, a_k, v_k, $\rho_{\text{air},k}$, and $C_{\text{d},k}$ represent the *mass*, the *acceleration*, the *velocity*, the *air density*, and *the drag coefficient* of EV k, respectively. Given EV k's battery power $P_{\text{batt},k}(t-1)$ at the time $(t-1)$, its battery power at time t is calculated by:

$$P_{\text{batt},k}(t) = P_{\text{batt},k}(t-1) + \frac{P_{\text{add},k}(t)}{\eta_{\text{wpt}}} - P_{\text{trac},k}(t), \tag{11}$$

where $P_{\text{add},k}(t)$ represents the *power added to EV k's battery at time t* and η_{wpt} represents the *wireless power transmission efficiency*. We can use Equation (11) to calculate power stored in the battery of EV of each time period based on the received energy, applied velocity, and acceleration. For an EV, when the brake is applied, $P_{trac,k}$ in Equation (11) becomes negative and its battery is charged by $P_{trac,k}$ amount of power at each time period.

Using Equation (10), we can predict the energy consumption rate of an EV considering different values of average velocity, average acceleration, and possible road gradients. More specifically, using Equations (8), (9), and (10) and the total length of the road section, we can compute the approximate energy consumption of an EV to cross a given road section. In addition, based on the average velocity for

a road section, we can estimate the travel time to cross that road section. For the sake of simplicity, we consider constant average velocity for a road section.

After the approximate energy and travel time estimations for different routes of an EV are determined, the proposed MORP system can choose the best possible route considering four factors discussed in the next section.

3.5 Optimal Routing Problem Formulation and Solution

Here, the goal is to find the optimized routing path for each EV to minimize energy consumption, travel time, charging monetary cost, and range anxiety *w.r.t.* different traffic scenarios. First, we introduce the maximum regret criterion to consider different traffic scenarios. Then, we present four different objective functions and formulate the EV routing problem as a multi-objective integer programming problem. Finally, we present the solution of the multi-objective optimization problem using the adaptive epsilon-constraint method [28].

3.5.1 Maximum regret criterion. As mentioned in Section 3.4, we consider three different velocity profiles (speed limit and positive and negative deviations from free-flow velocity) for the road sections at the same time. In this way, we can consider possible different traffic scenarios at the same time. One of these three velocity profiles for a road section would represent the worst conditions *w.r.t.* different factors (i.e., energy consumption, travel time, etc.) of an EV in that road section. Our goal is to choose the best possible path in the worst conditions. We consider the regret criterion so that the shortest path is robust enough [17]. Here, we incorporate regret as different traffic scenarios in the objective functions to choose the robust solution (i.e., best possible solution in the worst conditions). Each EV, say k, has different paths from source location to destination location which can be considered as a set of valid paths $\mathcal{C}_k$ from source location to the destination location. Let $\mathcal{S}$ represent the set of finite traffic scenarios based on the velocity profiles, $\tau^k_{i,j}$ represent a path from location i to location j for EV k, and $c^s(\tau^k_{i,j})$ represent its associate cost (e.g., energy consumption or traveling time) for scenario s. Similarly, let denote $\tau^{k,*}_{i,j}$ represent the shortest path from location i to location j for EV k and $c^s(\tau^{k,*}_{i,j})$ represent its associated cost. Let υ^k_{reg} denote the maximum regret for EV k considering worst and best scenarios. Then, the optimum solution according to the maximum regret criterion for an EV k is denoted as follows:

$$\upsilon^k_{reg}(\tau^{k,*}_{reg}) = \min_{\mu \in \mathcal{C}_k} \max_{s \in \mathcal{S}} c^s(\tau^k_{i,j}) - c^s(\tau^{k,*}_{i,j}), \tag{12}$$

where $\upsilon^k_{reg}(\tau^{k,*}_{reg})$ is the optimal solution according to the maximum regret criterion and cost function $c^s(\cdot)$. Thus, we can find a best available routing solution *w.r.t.* all possible traffic scenarios using maximum regret criterion.

3.5.2 Multi-objective optimization problem. We express four different criteria as four different cost functions and formulate a multi-objective optimization problem. We aim to minimize the travel time, energy consumption, range anxiety, and the charging monetary cost. Basically, we derive four different objective functions based on four different cost functions. Let $b^k_{i,j}$ denote a decision variable for an edge $e_{i,j}$ and path τ^k as follows:

$$b^k_{i,j} = \begin{cases} 1, & \text{if } e_{i,j} \in \tau^k \\ 0, & \text{if } e_{i,j} \notin \tau^k \end{cases} \tag{13}$$

where $b^k_{i,j}$ states if edge $e_{i,j}$ is included in path τ^k or not. Based on the maximum regret criteria (Equation (12)) and decision variable $b^k_{i,j}$, we formulate the multi-objective routing problem as an integer-programming problem.

First, we define the energy requirements of different edges of the road network *w.r.t.* different traffic scenarios (or velocity profiles). Let $\mathcal{E}_{i,j}^{s,k}(t)$ denote the energy cost of vehicle k for an edge $e_{i,j}$ at time t based on the scenario s. $\mathcal{E}_{i,j}^{s,k}$ can be calculated using Equation (10). Thus, the energy consumption cost function for all EVs can be defined as follows:

$$f_1^{\mu,s}(t) = \sum_{k \in K} \sum_{i,j \in V, i \neq j} \mathcal{E}_{i,j}^{s,k}(t) b_{i,j}^k. \tag{14}$$

Second, we consider the travel time of EV k. We use $\mathcal{R}_{i,j}^{s,k}(t)$ to denote the time for EV k to traverse edge $e_{i,j}$ at time t based on the scenario s. $\mathcal{R}_{i,j}^{s,k}$ can be calculated based on the length of the road section and predicted average velocity of a scenario (Equation (9)). We can express the travel time cost function for all EVs as follows:

$$f_2^{\mu,s}(t) = \sum_{k \in K} \sum_{i,j \in V, i \neq j} \mathcal{R}_{i,j}^{s,k}(t) b_{i,j}^k. \tag{15}$$

Third, we consider the charging monetary cost to choose some specific charging sections installed on the edges of the road network. Here, we consider charging sections are static and there are few charging sections installed on the edges of the road network. Usually, the marginal energy cost from the grid is spatio-temporal [4, 38] and the charging monetary costs at different charging sections are different. In addition, the total energy received from a charging section (or charging monetary cost) would be changed due to traffic flow rate. Thus, the idea is to choose other alternative edges to reduce the charging monetary cost. Let $r_{i,j}(t)$ represent the price of electricity rate for an edge $e_{i,j}$ at time t. Then, based on scenario s on a charging lane of an edge $e_{i,j}$, let EV k receive total $\mathcal{M}_{i,j}^{s,k}(t)$ amount of energy from the charging section installed in edge $e_{i,j}$ at time t. If there is no charging section in edge $e_{i,j}$, $\mathcal{M}_{i,j}^{s,k}(t)$ will be zero. $\mathcal{M}_{i,j}^{s,k}(t)$ can be calculated based on the length of the charging section, power transfer rate, and average velocity of a traffic scenario. This formulation will work perfectly with the consideration of a fixed charging monetary cost throughout the whole region. Eventually, we can formulate the third cost function of all EVs as follows:

$$f_3^{\mu,s}(t) = \sum_{k \in K} \sum_{i,j \in V, i \neq j} \mathcal{M}_{i,j}^{s,k}(t) rate_{i,j}(t) b_{i,j}^k. \tag{16}$$

Fourth, we consider range anxiety associated with the limitations of batteries used in EVs. The range anxiety actually depends on the current onboard energy and required energy to finish the whole trip. The WPT system would help to alleviate the range anxiety but it would take some time to overcome the range anxiety. Besides, unexpected traffic congestion and traffic signs at different road sections increase sudden changes of velocity. As a result, it is possible to increase unexpected energy consumption and range anxiety would be increased in these scenarios. Here, we treat the range anxiety as five different scales and we use a well-known rating scale model [18] to evaluate the range anxiety of commuters. If the difference between required energy to finish the trip and onboard energy stored in the battery is larger, range anxiety of commuters would increase gradually and vice versa. For edge $e_{i,j}$, we evaluate the probability of having range anxiety α (scales from 1 to $\mathcal{A}$) of the commuters of EV k based on its current SOC $y_k(t)$ and remaining required SOC $y_k^{req}(t)$ at time t as follows [18]:

$$P(\mathcal{A}_k = \alpha) = \frac{e^{\sum_{d=1}^{\alpha}(y_k(t) - \frac{y_k^{req}(t)}{y_k(t)} - \gamma_d)}}{\sum_{p=1}^{\mathcal{A}} e^{\sum_{d=1}^{p}(y_k(t) - \frac{y_k^{req}(t)}{y_k(t)} - \gamma_d)}}. \tag{17}$$

Table 3. Symbols and Definitions used in the optimization problem.

Notation	Definition
$\mathcal{C}_k$	The set of paths for EV k
$\mathcal{S}$	The set of scenarios
τ_k	A path for EV k
$c^s(.)$	Associated routing cost considering scenario s
υ^k_{reg}	Maximum regret criteria of EV k
$b_{i,j}$	Decision variable for an edge $e_{i,j}$
$\mathcal{E}_{i,j}$	Energy cost for edge $e_{i,j}$
$\mathcal{R}_{i,j}$	Traveling time for edge $e_{i,j}$
$r_{i,j}$	The price of energy for edge $e_{i,j}$
$\mathcal{M}_{i,j}$	Total amount of energy on edge $e_{i,j}$
α^k	Range anxiety of EV k
$\mathcal{A}$	Maximum anxiety level
f_i	i_{th} cost function
Υ_k	Power of EV k

Here, γ_α is the cut-off value of the range anxiety scale α which states as follows: SOC value in the range [0.0–0.2] for range anxiety scale 1, SOC value in the range [0.2–0.4] for range anxiety scale 2, and so on. Thus, we can decide the range anxiety $\alpha^{s,k}_{i,j}(t)$ for an edge $e_{i,j}$ at time t *w.r.t.* scenario s based on Equation (17). We can design the fourth cost function for all EVs as follows:

$$f_4^{\mu,s}(t) = \sum_{k\in K} \sum_{i,j\in V, i\neq j} \alpha^{s,k}_{i,j}(t) b^k_{i,j}. \tag{18}$$

Then, we can apply the above four cost functions in Equation (12) and get four objective functions $f_1^{\mu_{reg}}(\cdot)$, $f_2^{\mu_{reg}}(\cdot)$, $f_3^{\mu_{reg}}(\cdot)$, and $f_4^{\mu_{reg}}(\cdot)$ which basically consider maximum regret criteria *w.r.t.* different traffic scenarios. Eventually, we can formulate the following multi-objective optimization problem:

$$\min(f_1, f_2, f_3, f_4) \tag{19}$$

subject to:

$$b^k_{i,j} = \{0, 1\},\ \forall i, j, k \tag{20}$$

$$\sum_{k=1} \mathcal{M}^{s,k}_{i,j}(t) \leq cap_j,\ \forall k, j, t \tag{21}$$

$$y_k(t) \geq p_{\text{th},k},\ \forall t, k \tag{22}$$

$$y_k(t) \leq 1,\ \forall t, k \tag{23}$$

$$\Upsilon_k(t+1) = \begin{cases} \Upsilon_k(t) - P_{\text{trac},k} \\ \Upsilon_k(t) + \frac{\mathcal{M}_j(t)}{\eta_{\text{WPT}}} - P_{\text{trac},k} \end{cases} \tag{24}$$

where the first constraint (Equation (20)) represents the valid input of decision variable b. The second constraint (Equation (21)) means that the total power allocated to all EVs cannot exceed the maximum power provided by the charging section j. The third constraint (Equation (22)) means that the SOC of each EV k should be at least $p_{\text{th},k}$, which is a predetermined threshold for the SOC in each time point. The fourth constraint (Equation (23)) means that the SOC of each EV k cannot exceed 1 and the fifth constraint (Equation (24)) means that at time t, 1) if EV k is not located at any charging section, then its onboard energy is reduced by $P_{\text{trac},k}$ at each time unit; 2) if EV k is located at the charging section j, then its energy is added by $(\frac{\mathcal{M}_j(t)}{\eta_{\text{WPT}}} - P_{\text{trac},k})$ at each time unit. Table 3 shows the parameters related with the multi-objective optimization problem and its solution. Here, these four objective functions are not positively related with each other. For example, from Equation (10), f_1 increases

when f_2 decreases and vice versa. Also, f_2 is not always linear with f_3 as charging monetary costs at different charging sections would be different. f_4 mostly depends on required energy to finish the trip and current onboard energy of EVs. Next, we present the solution approach of the multi-objective problem.

ALGORITHM 1: Pseudocode for adaptive epsilon constraint method.

```
   Input: E = {}, N = {}, e = ((), (), ())
 1 Find the shortest paths for objective functions f_1, f_2, f_3, and f_4 and update e accordingly
 2 i ← 0
 3 h ← 1
 4 while true do
 5     while i ≤ h do
 6         (ϵ, ϵ́) ← getConstraints(m, e, |E|)//retrieve ϵ-constraints from matrix of coordinates e
 7         if [ϵ, ϵ́] ⊄ N then
 8             n ← opt(f, ϵ, ϵ́ )
 9             if n = null or ∃ń ∈ E : ń ≻ n then
10                 N ← N ∪ [ϵ, ϵ́]
11             end
12             else
13                 break
14             end
15             i ← i + 1
16         end
17     end
18     E ← E ∪ {n}
19     N ← N ∪ [f(s), ϵ́]
20     e ← updateConstraints(f(s), e)//update matrix of coordinates e and divide the grid
21     h ← (|E| + 1)^3
22     i ← 0
23 end
24 return E
```

3.5.3 Optimization problem solution. To solve the above optimization problem, we use the adaptive epsilon constraint framework. Basically, this framework alternates the multi-objective optimization problem into a single hyper-grid searching problem and it treats each objective function separately [28]. Algorithm 1 shows the overall procedures of the solution. Based on the number of objective functions, our multi-objective optimization problem turns into a 3-dimensional hyper-grid searching problem. Here, each dimension in the grid represents the constraint search space for each objective function, where $opt(f, \epsilon, \acute{\epsilon})$ returns the solution of the optimization problem based on the set of objective functions f, as well as ϵ and $\acute{\epsilon}$ as lower and upper bounds of the objective functions f. Here, we extend the original framework to increase the searching efficiency. At the beginning, we solve the single objective optimization problem for each objective function separately and find the shortest path for all four objective functions (f_1, f_2, f_3, and f_4) individually (Step 1). The values of these shortest paths are set as the lower limits ($\acute{\epsilon}$) of the objective functions. Then, we initially consider one objective function as the base objective function, whose objective space is dense. We utilize the remaining three objective functions where the grid cell coordinates are identified by the solutions of these objective functions. Thus, the whole potential objective space is $\mathbb{R}^4$. Here, we let define E as the already found solutions of the optimization problem and N as the already covered search space. We also define matrix E as the coordinates of the grid includes already found optimization solutions of f_1, f_2, and f_3, separately. After the initialization, at each step, we try to find a new solution (Step 4 - Step 23). More specifically, each time a new optimization solution is

Table 4. Parameters of Spark EV.

Descriptions	Values
Mass, M	1300 kg
Air density, A_f	1.97 m^2
Drag coefficient, C_d	0.33
Rolling resistance efficiency, μ	0.018
Power transforming efficiency, η_1	0.9
Powertrain working efficiency, η_2	0.97

sought using $opt(f, \epsilon, \acute{\epsilon})$ procedure (Step 8) based on the constraints $[\epsilon, \acute{\epsilon}]$ derived by *getConstraints(...)* procedure [28]. At first, $[\epsilon, \acute{\epsilon}]$ is derived (Step 6) and checked with the already covered search space N (Step 7). If $[\epsilon, \acute{\epsilon}]$ is completely new search space, a new solution n is generated using $opt(f, \epsilon, \acute{\epsilon})$ (Step 8). Then, n is compared with already found solutions set E (Step 9) and added to the set N if n does not dominate the solution set E (Step 10). Otherwise, a new solution is found and n is added to solution set E (Step 18). Then, $[\epsilon, \acute{\epsilon}]$ is added to the already covered search space, N (Step 19). $[\epsilon, f(A)]$ is added to the matrix e (Step 20) where 3-dimensional grid coordinates is divided based on *updateConstraints(...)* [28]. Finally, the number of cells is increased by the power of 3 (i.e., the number of objective functions minus one) (Step 21). The algorithm convergences to the Pareto front solution [27, 42] *w.r.t.* the number of solutions found and the number of objective functions (discussed in Appendix B).

4 PERFORMANCE EVALUATION

In this section, we evaluate the performance of proposed solutions in different aspects: vehicle count predictions at locations with/without historical traffic data, hourly average velocity and energy consumption predictions, the solution of proposed multi-objective optimization problem, and the impact of hourly average velocity prediction in the route planning. At first, we present the experimental settings used in different scenarios. Then, we present the experimental results with appropriate figures and descriptions.

4.1 Experimental Settings

4.1.1 Energy consumption rate. We built the energy consumption model based on the parameters of Chevrolet Spark EV (which has become popular recently [5]). Using the proposed energy consumption model, it is possible to calculate the energy consumption in different traffic scenarios (i.e., velocity values). From the Spark EV specifications, the battery pack structure consists of 2090 Sony VTC4-1850 Lithium-ion battery cells. Thus, the total capacity of the battery pack is 46.2 Ah and the voltage is 399 V. The rest of EV parameters are presented in Table 4.

4.1.2 Vehicle count prediction. For the traffic prediction estimation, we used our collected data from SC DOT. As stated before, we manually collected the historical traffic data from SC DOT web site for 212 days (December 1, 2016 – June 30, 2017). Initially, we choose 20 different traffic locations as shown in Fig. 3 to collect the data. Then, we used this data to estimate the parameters of our prediction models. Basically, the predictions for vehicle counts are divided into two categories. First, in the traffic locations with available data, we implemented the proposed horizontal ARIMA model using R. We used collected vehicle counts to estimate the parameters of the proposed horizontal ARIMA model. In the proposed horizontal ARIMA model, we fed the vehicle counts *w.r.t.* the hourly time of the day (e.g., 9 am, 10 am, and so on). We set both autoregressive (p) and moving average (q) parameters to 10 based on autocorrelation and partial autocorrelation functions. Figure 10 shows the autocorrelation and partial autocorrelation functions using vehicle counts in a traffic location (id 0086). We can see that both autocorrelation and partial autocorrelation values significant at time lag 10. For the comparison, we use existing (10,10) ARIMA model [12]. Second, in the case of the traffic locations without any historical data,

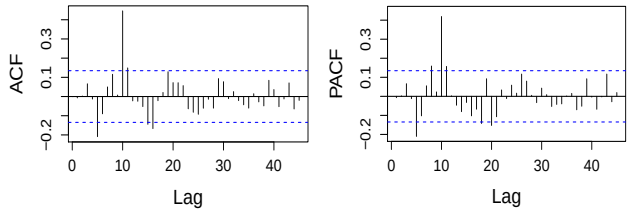

(a) Autocorrelation (b) Partial autocorrelation

Fig. 10. Correlation analysis of vehicle counts.

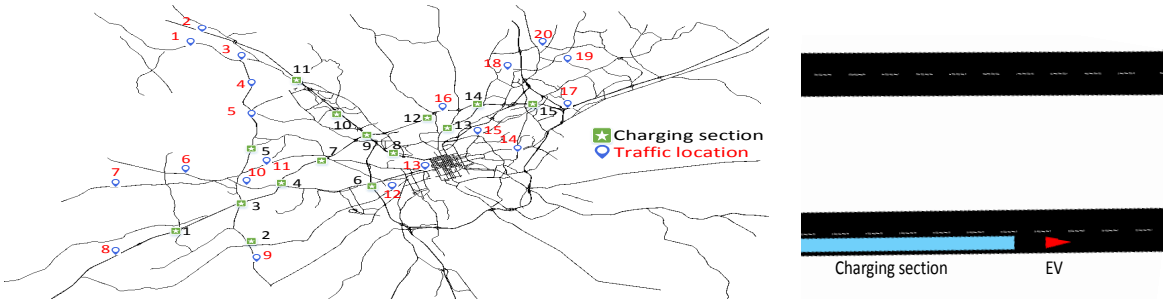

(a) Map (b) wireless charging section

Fig. 11. SUMO experiments.

we implemented spatio-temporal ordinary kriging using R. Initially, we utilized collected vehicle counts at 20 traffic locations. Ordinary kriging requires intermediate distance information of locations with historical data. Here, we used global positioning system (GPS) coordinates of these 20 traffic locations as GPS coordinates are more accurate spatial information. Then, we built and trained the ordinary kriging model using collected vehicle count values.

4.1.3 Average velocity prediction. Here, we implemented the kernel regression method using R to predict average velocity. We used the same collected traffic data to train kernel regression model. As a kernel function $K(\cdot)$ was set to the Gaussian function. The bandwidth value h was set to 0.63 based on the smoothness [45].

4.1.4 Multi-objective route planner. In this experiment, we first implemented our adaptive epsilon constraint method using python programming language. Then, we used the SUMO traffic simulator to verify the performances in real traffic scenarios. At first, we downloaded the road network map (included mostly highways) from OpenStreetMap and then, converted it into a bi-directional graph using NetworkX interface [3]. For each edge of the graph, we calculated the travel time and energy consumption using predicted vehicle counts and hourly average velocity. Particularly, we used Equation (9) and Equation (10) with the total length of an edge to calculate the travel time and energy consumption of that edge, respectively. In the experiments, we used 10 EVs and set the number of charging sections to 15 and we distributed these charging sections randomly to crowded road sections as shown in Figure 11(a). We randomly selected a value in [0.4,0.9] as the SOC for each EV when it enters the road network. We set each charging section length L and the maximum power capacity *cap* to 200 m and 500 kW, respectively. The amount of power each EV can receive is equal to the time it would spend on top of the charging section and it is directly related to the velocity of the EV. We used Equation (16) and Equation (18) to calculate the charging monetary cost and range anxiety of each individual EV, respectively. Figure 11(a) shows the SUMO network map converted from OpenStreetMap where each junction or point represents

Table 5. List of source-destination pairs.

EV	Source	Destination	EV	Source	Destination
1st	1	13	6th	19	2
2nd	16	10	7th	4	9
3rd	6	17	8th	18	8
4th	12	5	9th	14	3
5th	11	15	10th	7	20

node and each edge is represented by connecting the path between two nodes. The scaling of the map is 30 km×20 km. Figure 11(b) shows an EV leaving the wireless charging section in SUMO. Table 5 shows the source-destination pairs for 10 EVs *w.r.t.* different traffic locations.

Then, we solved the multi-objective optimization problem and obtained different optimal routes for different EVs. These routes were later used in SUMO to evaluate the performance in real traffic scenarios. More specifically, we utilized TraCI interface (included in SUMO) to route each vehicle from the source location to the destination location. We generated the hourly traffic flow in SUMO by setting the hourly number of vehicles traversing in each road section. To evaluate our performance in different scenarios, we conducted the experiments of multi-objective route planner in three different cases: first, we set 10 source-destination pairs for 10 EVs and ran the algorithm using the road network as shown in Figure 11(a). Here the number of charging sections is 15. Second, we removed six charging sections (#4, #7, #8, #9, #10, and #12) and ran the experiments again. Third, we further removed three edges between different charging sections [(#4, #6), (#4, #7), and (#9, #12)] and again ran the experiments. Finally, to verify the effectiveness of our method, we compared our optimization results with two other methods: one is the lexicographic solution approach used in [15] and another is EcoDrive, an existing energy efficient routing solution [24]. First, the lexicographic approach is applicable for solving any multi-objective optimization problem, different objective functions are solved separately and, finally, some additional constraints are added with each objective function to treat these objective functions together and find a solution satisfy each objective function. Second, EcoDrive focuses a single objective and it tries to reduce the fuel consumption of traditional vehicles *w.r.t.* the path length. To implement EcoDrive in terms of EVs, we mainly calculated total energy consumption (using Equation (10)) and used dynamic programming to find the most appropriate route such that total energy consumption is minimized. Here, we used the first experimental scenario as described above.

4.1.5 Impact of average velocity prediction in route planning. To evaluate the impact of hourly average velocity prediction in the route planning, we conducted an experiment in a route between charging section #7 and charging section #9. We let one EV drive from charging section #7 to charging section #9. The length of the route is 4.52 km and we considered the actual velocity of the route was 65 mph. We set the SOC of the EV to 0.45 and we assumed the EV drove the whole route smoothly. Here, we changed the error rate of average velocity prediction from -15% to +15% with 5% step size. Thus, there were seven cases in total. As usual, we calculated the energy consumption and SOC of the EV using Equation (10) and Equation (11), respectively. Also, we determined the charging monetary cost and range anxiety using Equation (16) and Equation (18), respectively.

4.2 Experimental Results

4.2.1 Energy consumption rate. Based on the proposed model, the energy consumption rate (in $mAhs^{-1}$) of the EV is shown in Figure 12 *w.r.t.* different values of velocity and acceleration. For simplicity, we consider the road gradient is zero. Here, velocity changes from 0 ms^{-1} to 35 ms^{-1} and acceleration changes from -2 ms^{-2} to 3 ms^{-2}. From the above figure, we can state that the energy consumption of an EV increases faster when it accelerates faster. We can also find that energy consumption of an EV is

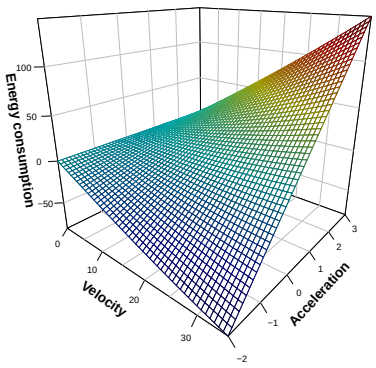

Fig. 12. Energy consumption rate.

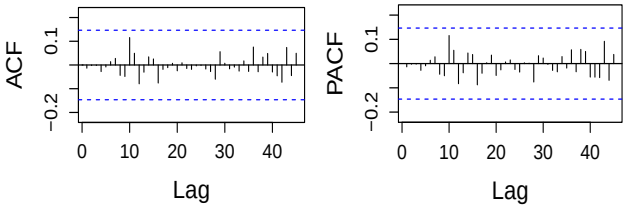

(a) Autocorrelation (b) Partial autocorrelation

Fig. 13. Correlation analysis of the proposed horizontal ARIMA model.

negative when the EV decelerates. It means the braking energy of EV would be able to transfer back into battery easily.

4.2.2 Vehicle count predictions. At first, we used the proposed horizontal ARIMA model to predict the vehicle counts in locations with historical traffic data. Figure 13 shows the correlation analysis of the proposed horizontal (10,10) ARIMA model for a randomly chosen location (id 0086) of the road network, where x axis shows the time lag and y axis represents autocorrelation or partial autocorrelation values, (autocorrelation and partial autocorrelation are explained in Section 3.3). From Figure 13(a) we can see that the model does not show any significant autocorrelations of the current vehicle count with the previous vehicle counts. It means our horizontal model predicts the vehicle counts accurately. Similarly, we can see from Figure 13(b) that there is no significant partial autocorrelation of current vehicle count with previous vehicle counts of the data. Above observations from Figure 13 verify the proper fitness of our model *w.r.t.* the collected data.

Figure 14 shows the proposed horizontal model prediction results based on the collected vehicle counts at the specific time of the day (9 am). Here x axis represents vehicle counts at the specific time of 212 days, y axis represents vehicle counts, darker shadow represents 80% confidence interval of predicted vehicle counts, and lighter shadow represents 95% confidence interval of predicted vehicle counts. We draw this figure using two different proposed (10,10) ARIMA models used for two different traffic locations. Figure 14(a) shows the prediction of vehicle counts at 9 am in another location (id 0086) and Figure 14(b) shows the prediction of vehicle counts at 9 am in another one location (id 0157). Both Figure 14(a) and Figure 14(b) show the predicted vehicle counts (blue line) and the actual vehicle counts (black line) are close to each other. Thus, we can again verify the prediction performance of the proposed horizontal ARIMA model. Next, Figure 15 shows the predicted and actual vehicle counts in one location (id 0086) for seven days (March 12 to March 18) where it snows on March 12 and March 16. We can see that the

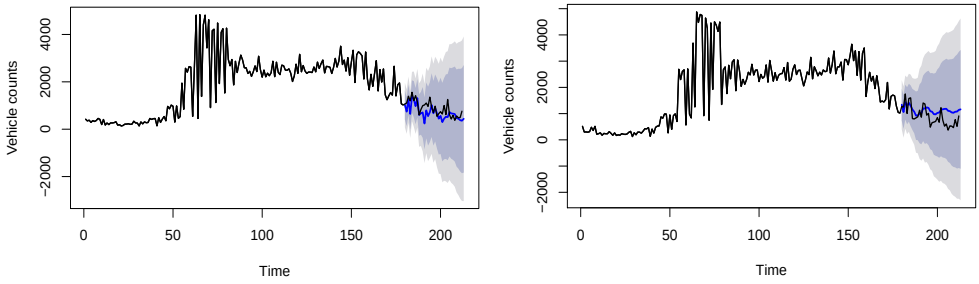

(a) ARIMA 1 (b) ARIMA 2

Fig. 14. Prediction using ARIMA model.

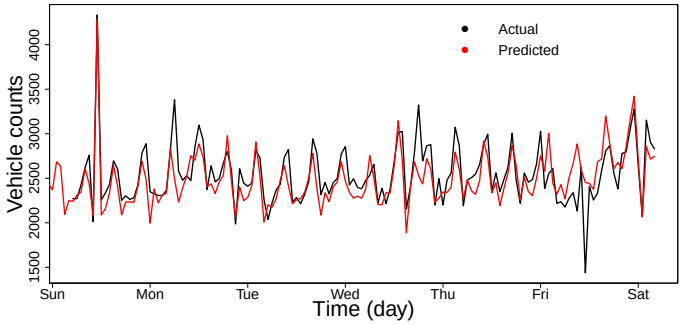

Fig. 15. Actual and predicted vehicle counts.

predicted vehicle counts almost overlap with the actual vehicle counts at different times of the day. It means that the proposed ARIMA model can predict the trends of vehicle counts throughout the day.

Then, we compare the performance of vehicle counts of the proposed ARIMA model and the existing (10,10) ARIMA model. Figure 16 basically shows the comparison of vehicle count predictions between the existing (10,10) ARIMA and the proposed horizontal (10,10) ARIMA in terms of Mean Absolute Error (MAE)and Root Mean Square Error (RMSE). Here, we use vehicle counts in 10 different traffic locations and a specific time of the day (12 pm). Using the RMSE value, we can analyze the deviation of the prediction from original data and MAE value can help us to interpret the prediction accuracy. Thus, we can analyze any traffic location (e.g., id 0001) and check the deviation and prediction error based on RMSE and MAE values of two models. For most of the locations, MAE and RMSE values are similar except for one location (id 0147) where that location does not have any neighbor and the vehicle counts of that location are skewed. In addition, the variance of the prediction errors of vehicle counts is larger and error magnitudes are in the same direction rather than in other locations. We can easily verify that the proposed horizontal ARIMA model is more accurate and deviates less from the original data. However, the existing ARIMA model produces more false predictions and the deviation from the original data is much higher. As we consider data-driven intubation to use horizontal historical data, the accuracy of our proposed ARIMA model is better. Also, instead of considering the average velocity of neighbor traffic locations, we consider the number of vehicles of neighbor points and it decreases the possible deviation from historical vehicle counts.

Now, in traffic locations without any historical traffic data, we used the ordinary kriging approach as shown in Figure 17 where x axis represents the intermediate distances between different traffic locations, y axis represents the time lag (interval between different times), and z axis represents the value of γ

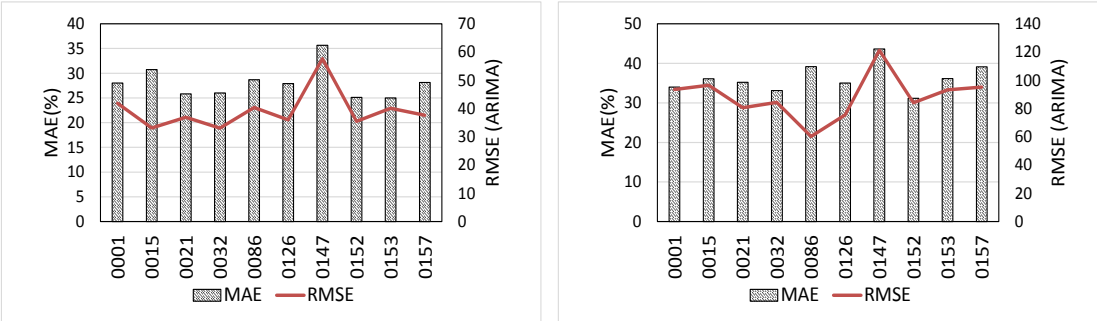

(a) Proposed model (b) Existing model

Fig. 16. The Comparison between existing and proposed (10,10) ARIMA models.

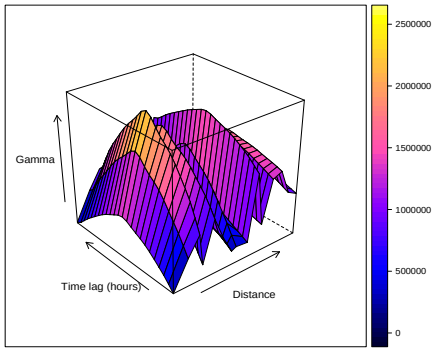

Fig. 17. Variogram.

function (Equation (7)). From this graph, we can estimate the vehicle counts using γ function *w.r.t.* any given location at a given time of the day.

4.2.3 Average velocity estimations. Figure 18 shows the hourly average velocity prediction using the kernel regression method. Here we consider two different cases: upper range of hourly average velocity prediction (*w.r.t.* the speed limit) and lower range of hourly average velocity prediction (*w.r.t.* the speed limit). More exactly, Figure 18(a) shows the lower range of hourly average velocity prediction using historical vehicle counts in a location (id 0086). Here, the hourly average velocity is less than the speed limit. x axis represents vehicle counts and y axis represents average velocity (in mph). We can see that initially hourly average velocity decreases when the vehicle count increases. However, when the vehicle count reaches around 1400, the average velocity starts to increase. There is another fall of the average velocity when the vehicle count reaches around 2500. Next, Figure 18(b) shows the upper range of hourly average velocity prediction *w.r.t.* vehicle counts in the same location. In contrast to the previous figure, here, the hourly average velocity is greater than the speed limit. We can see that initially hourly average velocity increases gradually when vehicle count increases. However, the average velocity decreases sharply when vehicle count is around 3500. However, average velocity reaches a steady state when vehicle count is more than 5000.

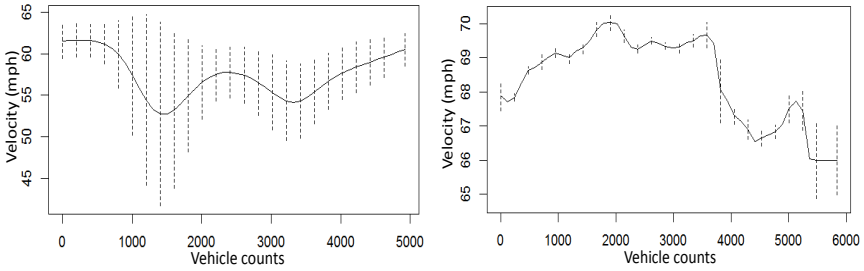

(a) Lower range (b) Upper range

Fig. 18. Prediction of hourly average velocity *w.r.t.* the speed limit.

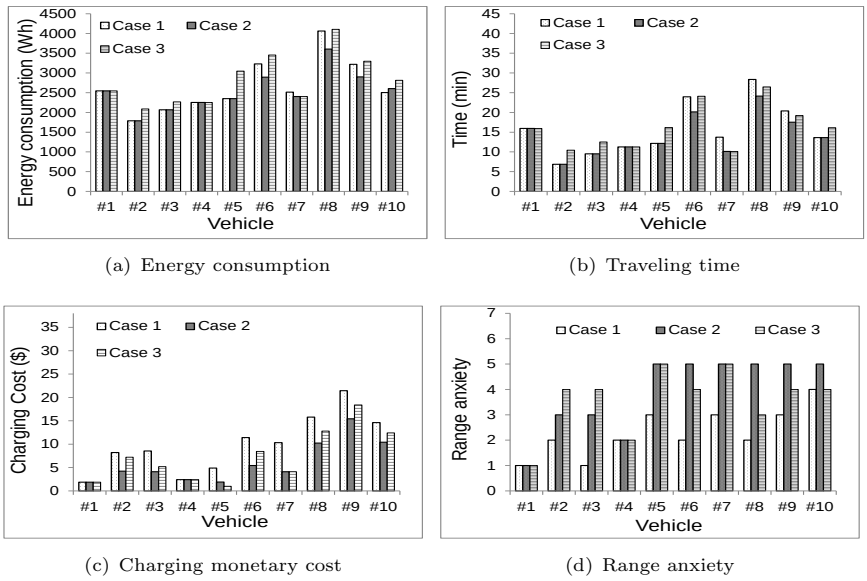

(a) Energy consumption (b) Traveling time

(c) Charging monetary cost (d) Range anxiety

Fig. 19. Vehicle routing results in three different cases.

4.2.4 Multi-objective optimization solutions. First, we evaluate the performances of our adaptive epsilon constraint approach in three different cases as described in Section 4.1.4. Figure 19(a) shows the corresponding energy consumption in three cases. We see that energy consumption of the 1st and 4th EVs are unchanged. Energy consumption of the 2nd, 3rd, and 5th are unchanged in the second case but increased in the third case. Also, energy consumption of the 6th, 8th, and 9th EV are decreased in the second case but are increased in the third case. The 7th EV's energy consumption is the same in the second and third cases, and finally, the 10th EV's energy consumption increases in the second and third cases. Similarly, Figure 19(b) shows the required travel time of EVs in three cases. Travel times of the 1st and 4th EVs remain unchanged in three cases. The 2nd, 3rd, and 5th EVs' travel times remain the same in the first two cases but increase in the third case. The travel times of the 6th, 7th, and 9th EVs are decreased in the second case but increased in the third case compared with the second case. The 7th EV's travel time is the same in the second and third cases. And, the travel time of the 10th EV is increased only in the third case. Then, Figure 19(c) shows the charging monetary cost of 10 EVs in three cases. As in the previous two figures, the charging monetary cost of the 1st and 4th EVs remain

unchanged. The charging monetary cost of the 6th, 8th, and 9th EVs are decreased in the second case but increased in the third case. The 2nd, 3rd, and 5th EVs' charging costs are decreased in the second and third case compared to the first case. The 7th EV's charging cost is the same in the second and third cases. The charging monetary cost of the 10th EV is also decreased in the second and third cases. And, Figure 19(d) shows the range anxiety of commuters of the 10 EVs in three cases. Similar to previous figures, the range anxieties of the 1st and 4th EVs remain the same. The 2nd, 3rd, and 5th EVs' range anxieties are increased in the second and third cases. The Range anxieties of the 6th, 8th, and 9th EVs are increased in the second case but decreased in the third case. The 7th EV's range anxiety is the same in the second and third cases. The 10th EV's range anxiety is the same in the first and third cases.

From the above discussion, it is obvious that the 1st and 4th EVs' routes do not affect the EVs at all in three cases (all four factors are remain the same). The 2nd and 3rd EVs' routes remain the same in the second case (same energy consumption and travel time but less charging cost) and they have to choose a new route in the third case (more energy consumption and travel time with more charging cost). The routes of EV 5 is the same in the first and second cases but it takes a new route with fewer charging sections in the third case. The routes of the 6th, 8th, and 9th EVs take a detour without these five removed charging sections in the second case (less energy consumption and charging cost with more anxiety) but have to choose a longer path with a new charging section in the third case. The 7th EV is not affected by edge removal and takes the same route in the second and third cases (same charging cost and range anxiety). The 10th EV takes the same route in the first and second cases but has to choose another route with a new charging section in the third case. Thus, we can state that it is not obvious that a new charging section in the road network would spur all EVs to change their routes in the adaptive epsilon constraint approach. This is because our adaptive epsilon constraint approach always tries to find a new Pareto optimal path [27, 42] which can satisfy all already found solutions.

Second, we evaluate the performance of our adaptive epsilon constraint approach by comparing with the lexicographic approach to solve the multi-objective optimization problem. We also compared our solution with another existing system, called EcoDrive which considers only energy efficiency as the singular objective function. Four different figures (in Figure 20) show the evaluation of three different solution approaches in four aspects: energy consumption, travel time, charging monetary cost, and range anxiety. First, Figure 20(a) shows the energy consumption amount of 10 different EVs based on the solution approaches used. Here, we calculate the energy consumption as the difference between previous onboard energy before starting the trip and current onboard energy after finishing the trip. We can see that the adaptive epsilon constraint method requires more energy than others as our adaptive epsilon constraint approach try to find a routing solution which considers all four objective functions together. In the lexicographic approach, some constraints of the objective functions are relaxed and this approach requires a modest amount of energy. EcoDrive requires the lowest amount of energy as it considers only energy efficient routing. Then, Figure 20(b) shows the travel time of 10 EVs using three different approaches with the same source-destination pairs. We calculated the travel time using total time to finish the trip, which also included the waiting time in front of traffic signals. Using the velocity profile of an EV over time, we can determine if the EV stops at the traffic signal and then calculate the waiting time. Here, we can see that EcoDrive requires the highest amount of time as it only considers energy consumption and sacrifices travel time. Then, the lexicographic approach requires the second greatest amount of travel time as it gives highest priority to the energy consumption factor. In our adaptive epsilon constraint approach, the required travel time is slightly lower than the lexicographic approach due to the consideration of the four objectives.

Figure 20(c) shows charging monetary cost of 10 EVs when three different solution approaches are used. The cost to charge the EVs is considered using randomly chosen unit electricity values for different

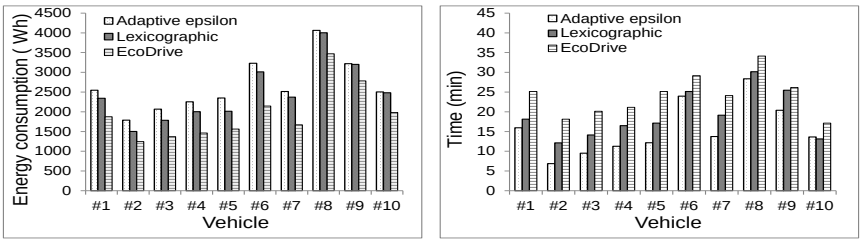

(a) Energy consumption

(b) Traveling time

(c) Charging monetary cost

(d) Range anxiety

Fig. 20. Vehicle routing results using three different optimization approaches.

subregions so that we would be able the evaluate the real grid scenario where the price of electricity is different in different regions due to the power fluctuations. Here, the charging cost in EcoDrive is highest as it always tries to find the path which requires the lowest onboard energy consumption. The charging cost in the lexicographic approach is modest as it considers charging cost as the third objective function. Here, the charging cost of the adaptive epsilon constraint method is lowest as our method has the consideration to balance different objectives. Finally, the range anxieties of 10 EVs commuters using three different approaches are given in Figure 20(d). Here, we calculate the range anxiety using Equation (17). We can see that the range anxiety of the commuters in our method is lower than in the other two methods. The main reason is that the other two methods either do not have any range anxiety consideration or give the lowest priority to the range anxiety.

From the above discussion, we can see that our adaptive epsilon constraint approach can offer a more balanced solution compared with the existing lexicographic approach and EcoDrive. The adaptive epsilon constraint method tries to find the balance between different objective functions and to find a routing path from source to destination which does not cause a much higher charging cost or higher range anxiety or higher traveling time. The performance of the lexicographic is worse *w.r.t.* the range anxiety and charging monetary cost minimization. Even though the energy consumption of the lexicographic method is lower than our method, the energy consumption differences are not significant (less than 10%). The trip time of the lexicographic approach is a little bit higher than our approach in most of the cases. Basically, the lexicographic approach relaxes some search spaces of objective functions and it tries to find an overlapping region among four different objective functions. In the case of EcoDrive routing solution, the travel time, charging cost, and range anxiety are almost always higher than in the other two approaches. Since EcoDrive only considers energy consumption in the optimization problem. EcoDrive cannot satisfy other objectives and its performance is worse than in the other two solution approaches.

4.2.5 Impact of average velocity prediction in route planning. Table 6 shows the impact of hourly average velocity prediction in route planning. Here, there are seven cases in total. We can see that the more positive error rate in hourly average velocity prediction causes more energy consumption of the EV and

Table 6. Impact of hourly average velocity prediction.

Error rate	Energy consumption	Travel time	Charging monetary cost	Range anxiety
(+)5%	833.11 kW	148.14 s	$ 1.78	3
(+)10%	914.34 kW	141 s	$ 1.75	3
(+)15%	999.35 kW	135.26 s	$ 1.70	4
0%	755.65 kW	155.4 s	$ 1.82	2
(-)5%	612.08 kW	163.2 s	$ 1.86	1
(-)10%	681 kW	172.83 s	$ 1.92	1
(-)15%	545.96 kW	183 s	$ 1.97	1

requires less travel time to finish the trip. As a result, the positive error rate in hourly average velocity prediction requires a lower charging monetary cost but causes more range anxiety. However, the more negative error rate in hourly average velocity prediction requires a higher charging monetary cost and causes less range anxiety. This is because the negative error rate requires more travel time and consumes more energy. From the above discussion, we can easily understand the importance of traffic predictions (i.e., vehicle counts or hourly average velocity) in route planning.

5 RELATED WORK

Vehicle routing. The traditional vehicle routing problem is studied by several existing works [9, 19, 40, 56] where the main idea is to distribute the vehicles among road networks satisfying energy constraints of vehicles. In addition, different other aspects (e.g., traveling time, load distribution, road network utilization, etc.) are considered as the cost functions. As an example, Goseiri et al. [19] proposed a multi-objective optimization problem for taxis to minimize travel distance and serve more passengers. Another work by Banos et al. [9] tries to solve the vehicle routing problem in terms of minimizing distance traveled and balancing the workload (delivery services) of different vehicles with strict deadline constraints. The authors proposed a combination of evolutionary computation and simulated annealing approaches to solving the multi-objective formulations of the vehicle routing problem. A real-time congestion-aware vehicle routing problem is proposed by Zhang et al. [56] and the solution of a routing problem is established using the lexicographic approach. The main idea is to predict the flows of existing vehicles in the road network such that it: (i) transfers passengers to their destinations in minimum time and (ii) re-balances vehicles throughout the network to satisfy the passengers' demand of taxis. Similar to our routing problem, Schneider et al. [40] studied the EVs' routing problem to satisfy the charging schedules of stationary charging stations and to minimize energy consumption without using any multi-objective consideration.

In the routing of online EVs, it is important to ensure a sufficient power supply along the way and the commuter's range anxiety, charging monetary cost, travel time, and energy consumption should be considered together. Besides, the above studies, without leveraging the ubiquitous traffic flow patterns of the road network, may fail to validate in real-life scenarios. Our ubiquitous data-driven EV routing problem considers current traffic conditions to ensure the onboard energy constraints and consider multiple objectives to provide an optimal routing solution.

Data-driven intelligent transportation system. Utilizing the spatio-temporal features of road networks to ensure better travel experiences (safety, comfort, etc.) within the transportation system falls into the category of urban computing and has been studied in recent years [6, 7, 10, 26, 49–51, 54]. As an example, the existing study [32] is inspired to provide real-time route guidance utilizing the probability-based congestion awareness of real traffic analysis. A very common approach to this set of works is to predict the near-future traffic states based on available historical data. The study [7] utilizes periodic messages (containing the location, passenger status, destination, etc.) from taxis to generate current traffic snapshots and provide accurate traffic forecasting based on previous taxis' trajectories. Another work [10] analyzes the intra-day trends for traffic flow series to improve the prediction of vehicular congestion. Xu et

al. [49] proposed a framework for online traffic prediction leveraging contextual correlation of predictors. In their work, several weak predictors are dynamically adjusted to build a strong self-adapting hybrid predictor.

Abadi et al. [6] designed a traffic simulator based on an autoregressive prediction algorithm to be more adaptable to the unpredictable events. Zhang et al. [54] combined several traffic datasets to design a data-driven service to notify commuters about possible stop location and departure time. Another data-driven system DESTPRE [50], predicts the destination of a partial trajectory based on the similarity between different vehicles' trajectories. Ziebart et al. [59] utilized context-aware user behaviors and context-sensitive action utilities towards vehicle route preference modeling to predict left and right turns, traversing the path and final destination of vehicles. De et al. [14] presented a probability-based intention aware routing of EVs considering waiting time reduction in static charging stations. Also, Sun et al. [43] integrated predictive hybrid-EV energy management strategy with real-time vehicles' trajectory information to find out optimal SOC trajectory (SOC consumption profiles of the trajectory) using dynamic programming approach. The above data-driven existing works do not utilize spatio-temporal correlations of different traffic locations such that the computation complexity in vehicle routing problem would be reduced as it discards some repetitive steps. Although some of these works [14, 32, 43] utilize ubiquitous traffic patterns in vehicle routing problem, they ignore multiple aspects in the vehicle routing problem. For example, Yuan et al. [53] considered routing of individual vehicles based on the probabilistic prediction using hidden markov model and Horvitz et al. [21] considered opportunistic routing of different paths based on historic user preferences without having multiple objectives. In our work, we leverage spatio-temporal correlations of different nodes to reduce prediction complexity of vehicle routing problem to satisfy multiple objectives.

6 CONCLUSIONS

In this paper, we proposed MORP, a ubiquitous data-driven route planner of online EVs consisting of four different factors (travel time, energy consumption, charging cost, and range anxiety). We first conducted ubiquitous traffic flow data analysis and found the spatial-temporal features of vehicle counts and velocity. Based on our observations, we built several models to predict vehicle counts and average velocity. MORP system predicts the vehicle counts using the proposed horizontal ARIMA model and the ordinary kriging model for locations (both) with and without traffic data. Then, it predicts the average velocity of each road section using non-parametric kernel repression along with predicted vehicle counts. Again, MORP predicts travel time using the predicted average velocity of each road section. Finally, it predicts energy consumption of different road sections using a proposed energy consumption model with the help of predicted average velocity of these road sections. Eventually, predicted travel time and energy consumption are used as the inputs of two cost functions in the multi-objective optimized routing solution. We also considered charging monetary cost and range anxiety of EVs as two other cost functions in the routing solution. Basically, we applied the adaptive-epsilon constraint method along with a robust optimization technique in order to obtain the solution of the multi-objective optimization problem of the best available routes for different EVs. As a result, the proposed MORP system offers several optimal routes in the road network while minimizing travel time, energy consumption, charging monetary cost, and range anxiety of EVs. We evaluated the proposed MORP system using different experimental tools in order to consider different scenarios. Most importantly, we evaluated the performances along optimized routes using SUMO traffic simulator to check the validity of proposed MORP in real traffic scenarios. In the future, we would like to devise more sophisticated regression models in traffic predictions and build an online optimization framework based on more complex traffic scenarios.

A PARAMETERS ESTIMATION FOR HORIZONTAL ARIMA MODEL

First, we derive the log likelihood function of the distribution of vehicle counts using autocorrelation function of its time series. Then, we design a minimization problem to estimate the values of all parameters in Equation (3) (except p, q, and W).

Let Γ_i represent the autocovariance function of the vehicle counts x at time t. Then, we can write:

$$\Gamma_i = E[x(t), x(t-i)], \tag{25}$$

where E is the expected value of the vehicle counts $x(t)$. Equation (25) can be further used to represent the autocorrelation function ρ_i, the covariance at time lag i divided by the variance of the vehicle counts. Thus, it can be written as follows:

$$\rho_i = \frac{\Gamma_i}{\Gamma_0} \tag{26}$$

Now, if we consider proposed horizontal ARIMA model is basically a zero mean Gaussian process. Then for any fixed value θ, ψ, Θ, Ψ, and σ^2, the $(x_1 - \bar{x_1})$, ..., $(x_n - \bar{x_n})$ are independent and normally distributed with variances $\sigma^2\rho_0$, ..., $\sigma^2\rho_{n-1}$. Then, the likelihood function can be written as:

$$L(\theta, \psi, \Theta, \Psi, \sigma^2) = \prod_{i=1}^{n} \frac{1}{\sqrt{2\pi\sigma^2\rho_{i-1}}} exp\Big\{ - \frac{(x_i - \bar{x_i})^2}{2\sigma^2\rho_{i-1}} \Big\} \tag{27}$$

Now, if we apply log in Equation (27), we can get the following form:

$$lnL(\theta, \psi, \Theta, \Psi, \sigma^2) = -\frac{1}{2}((2\pi\sigma^2)^n\rho_0...\rho_{n-1}) - \frac{S(\theta, \psi, \Theta, \Psi)}{2\sigma^2}, \tag{28}$$

where $\frac{S(\theta,\psi,\Theta,\Psi)}{2\sigma^2} = \sum_{i=1}^{n} \frac{(x_i - \bar{x_i})^2}{\rho_{i-1}}$. Next, by differentiation of Equation(29) *w.r.t.* to σ^2, we can get following minimization problem:

$$lnL(\theta, \psi, \Theta, \Psi) = ln(\frac{S(\theta, \psi, \Theta, \Psi)}{n}) + \frac{\sum_{i=1}^{n} ln\rho_{i-1}}{n}(2\pi\sigma^2)^n\rho_0...\rho_{n-1}) - \frac{S(\theta, \psi, \Theta, \Psi)}{2\sigma^2}, \tag{29}$$

which can be done numerically using Newton-Raphson's method [8].

B CONVERGENCE OF PARETO OPTIMALITY OF MULTI-OBJECTIVE OPTIMIZATION

THEOREM B.1. *If $|F|$ is the number of objective functions and k is the number of times that the single-objective optimizer will be called, then the complexity of Algorithm 1 to discover a Pareto optimal solution is $O(|k|^3)$.*

PROOF. The single objective optimizer, *opt(...)* is called for different combinations of upper and lower constraint vectors (ϵ,$\acute{\epsilon}$) (Step 8 in Algorithm 1). Each newly found solution leads to 3 new constraint values and further subdivision of some of the previous constraint regions. Given a constraint matrix e, the total number of times the algorithm calls the single objective optimizer equals $(|E| + 1)^3$ where $|E|$ is the total number of newly found solutions. E includes all and only Pareto optimal solutions which have not been either discovered or dominated by already found solutions. $|E|$ is maximal when all Pareto optimal solutions have been discovered and included in E, i.e., $f(E) = F^*$. Thus, the single objective optimizer can not be called for more than $(|F^*| + 1)^3$ and $k = |F^*| + 1$. It completes the proof. □

ACKNOWLEDGMENTS

The authors are grateful to the anonymous reviewers for their valuable suggestions. The authors would also like to thank Mrs. Martha Steele for her continuous support. This research was supported in part by U.S. NSF grants OAC-1724845, ACI-1719397 and CNS-1733596, Microsoft Research Faculty Fellowship 8300751, and IBM Ph.D. fellowship award 2017.

REFERENCES

[1] 2017. Hourly Traffic Data. (2017). http://www.dot.state.sc.us/ Accessed: May, 2017.
[2] 2017. INRIX Traffic Scorecard. (2017). http://inrix.com/scorecard/ Accessed: May, 2017.
[3] 2017. NetworkX Graph. (2017). http://networkx.readthedocs.io/en/networkx-1.10 Accessed: May, 2017.
[4] 2017. Pricing Data. (2017). http://www.nyiso.com/public/markets_operations/market_data/pricing_data/index.jsp Accessed: May, 2017.
[5] 2017. Spark Electriv Vehicle. (2017). http://www.chevrolet.com/spark-fuel-efficient-car Accessed: May, 2017.
[6] Afshin Abadi, Tooraj Rajabioun, and Petros A Ioannou. 2015. Traffic flow prediction for road transportation networks with limited traffic data. *IEEE Trans. on ITS* 16, 2 (2015).
[7] Javed Aslam, Sejoon Lim, Xinghao Pan, and Daniela Rus. 2012. City-scale traffic estimation from a roving sensor network. In *Proc. of ENSS*.
[8] Mordecai Avriel. 2003. *Nonlinear programming: analysis and methods*.
[9] RaúL BañOs, Julio Ortega, ConsolacióN Gil, Antonio L MáRquez, and Francisco De Toro. 2013. A hybrid meta-heuristic for multi-objective vehicle routing problems with time windows. *Computers & Industrial Engineering* 65, 2 (2013).
[10] Chenyi Chen, Yin Wang, Li Li, Jianming Hu, and Zuo Zhang. 2012. The retrieval of intra-day trend and its influence on traffic prediction. *Transportation research part C: Emerging Technologies* 22 (2012).
[11] Tao Cheng, Jiaqiu Wang, James Haworth, Benjamin Heydecker, and Andy Chow. 2014. A dynamic spatial weight matrix and localized space–time autoregressive integrated moving average for network modeling. *Geographical Analysis* 46, 1 (2014).
[12] Pierre A Cholette. 1982. Prior information and ARIMA forecasting. *Journal of Forecasting* 1, 4 (1982).
[13] Noel Cressie. 1988. Spatial prediction and ordinary kriging. *Mathematical geology* 20, 4 (1988).
[14] Mathijs M de Weerdt, Sebastian Stein, Enrico H Gerding, Valentin Robu, and Nicholas R Jennings. 2016. Intention-aware routing of electric vehicles. *IEEE Trans. on ITS* 17, 5 (2016).
[15] Kalyanmoy Deb, Karthik Sindhya, and Jussi Hakanen. 2016. Multi-objective optimization. In *Decision Sciences: Theory and Practice*.
[16] Yan Ding, Chao Chen, Shu Zhang, Bin Guo, Zhiwen Yu, and Yasha Wang. 2017. GreenPlanner: Planning personalized fuel-efficient driving routes using multi-sourced urban data. In *Proc. of PERCOM*.
[17] Matthias Ehrgott, Jonas Ide, and Anita Schöbel. 2014. Minmax robustness for multi-objective optimization problems. *European Journal of Operational Research* 239, 1 (2014).
[18] Gerhard H Fischer and Ivo W Molenaar. 2012. *Rasch models: Foundations, recent developments, and applications*. Springer Science & Business Media.
[19] Keivan Ghoseiri and Seyed Farid Ghannadpour. 2010. Multi-objective vehicle routing problem with time windows using goal programming and genetic algorithm. *Applied Soft Computing* 10, 4 (2010).
[20] Jeffrey D Hart and Thomas E Wehrly. 1986. Kernel regression estimation using repeated measurements data. *JASA* 81, 396 (1986).
[21] Eric Horvitz and John Krumm. 2012. Some help on the way: Opportunistic routing under uncertainty. In *Proc. of UBICOMP*.
[22] Shenggong Ji, Yu Zheng, and Tianrui Li. 2016. Urban sensing based on human mobility. In *Proc. of UBICOMP*.
[23] Malte F Jung, David Sirkin, Turgut M Gür, and Martin Steinert. 2015. Displayed uncertainty improves driving experience and behavior: The case of range anxiety in an electric car. In *Proc. of CHI*.
[24] Lei Kang, Bozhao Qi, Dan Janecek, and Suman Banerjee. 2015. EcoDrive: A Mobile Sensing and Control System for Fuel Efficient Driving. In *Proc. of Mobicom*.
[25] Daniel Krajzewicz, Jakob Erdmann, Michael Behrisch, and Laura Bieker. 2012. Recent Development and Applications of SUMO - Simulation of Urban MObility. *International Journal On ASM* (2012).
[26] John Krumm and Eric Horvitz. 2006. Predestination: Inferring destinations from partial trajectories. In *Proc. of UBICOMP*.

[27] Marco Laumanns, Lothar Thiele, Kalyanmoy Deb, and Eckart Zitzler. 2002. Combining convergence and diversity in evolutionary multiobjective optimization. *Evolutionary computation* 10, 3 (2002).
[28] Marco Laumanns, Lothar Thiele, and Eckart Zitzler. 2006. An efficient, adaptive parameter variation scheme for metaheuristics based on the epsilon-constraint method. *European Journal of Operational Research* 169, 3 (2006).
[29] I Lawrence and Kuei Lin. 1989. A concordance correlation coefficient to evaluate reproducibility. *Biometrics* (1989).
[30] Arthur Lewbel and Oliver Linton. 2002. Nonparametric censored and truncated regression. *Econometrica* 70, 2 (2002).
[31] Ruimin Li, Geoffrey Rose, and Majid Sarvi. 2006. Using automatic vehicle identification data to gain insight into travel time variability and its causes. *JTRB* 1945 (2006).
[32] Jie Lin, Wei Yu, Xinyu Yang, Qingyu Yang, Xinwen Fu, and Wei Zhao. 2015. A novel dynamic En-route decision real-time route guidance scheme in intelligent transportation systems. In *Proc. of ICDCS*.
[33] Jeremy Neubauer and Eric Wood. 2014. The impact of range anxiety and home, workplace, and public charging infrastructure on simulated battery electric vehicle lifetime utility. *Journal of Power Sources* 257 (2014).
[34] Chenxi Qiu, Ankur Sarker, and Haiying Shen. 2017. Power distribution scheduling for electric vehicles in wireless power transfer systems. In *Proc. of SECON*.
[35] Chenxi Qiu, Haiying Shen, Ankur Sarker, Vivekgautham Soundararaj, Mac Devine, and Egan Ford. 2016. Towards Green Transportation: Fast Vehicle Velocity Optimization for Fuel Efficiency. In *Proc. of IEEE CloudCom*.
[36] Nadine Rauh, Thomas Franke, and Josef F Krems. 2015. Understanding the impact of electric vehicle driving experience on range anxiety. *Human factors* 57, 1 (2015).
[37] Jackeline Rios, Pablo Sauras-Perez, Andrea Gil, Andre Lorico, Joachim Taiber, and Pierluigi Pisu. 2014. *Battery electric bus simulator-a tool for energy consumption analysis*. Technical Report. SAE Technical Paper.
[38] Ankur Sarker, Zhuozhao Li, William Kolodzey, and H. Shen. 2017. Opportunistic energy sharing between power grid And electric vehicles: A game theory-based nonlinear pricing policy. In *Proc. of ICDCS*.
[39] Ankur Sarker, Chenxi Qiu, Haiying Shen, Andrea Gil, Joachim Taiber, Mashrur Chowdhury, Jim Martin, Mac Devine, and AJ Rindos. 2016. An efficient wireless power transfer system to balance the state of charge of electric vehicles. In *Proc. of ICPP*.
[40] Michael Schneider, Andreas Stenger, and Dominik Goeke. 2014. The electric vehicle-routing problem with time windows and recharging stations. *Transportation Science* 48, 4 (2014).
[41] Liuwang Kang Haiying Shen and Ankur Sarker. 2017. Velocity optimization of pure electric vehicles with traffic dynamics and driving safety considerations. In *Proc. of ICDCS*.
[42] V Srinivasan and Gerald Luther Thompson. 1976. Algorithms for minimizing total cost, bottleneck time and bottleneck shipment in transportation problems. *Naval Research Logistics* 23, 4 (1976).
[43] Chao Sun, Scott Jason Moura, Xiaosong Hu, J Karl Hedrick, and Fengchun Sun. 2015. Dynamic traffic feedback data enabled energy management in plug-in hybrid electric vehicles. *IEEE Trans. on CST* 23, 3 (2015).
[44] Nick T Thomopoulos. 2015. Demand forecasting for inventory control. In *Demand Forecasting for Inventory Control*.
[45] Matt P Wand and M Chris Jones. 1994. *Kernel smoothing*. Crc Press.
[46] H. Wang, J. Gong, Y. Zhuang, H. Shen, and J. Lach. 2017. Healthedge: Task scheduling for edge computing with health emergency and human behavior consideration in smart homes. In *Proc. of Big Data*.
[47] Xiaokun Wang and Kara Kockelman. 2009. Forecasting network data: Spatial interpolation of traffic counts from texas data. *JTRB* 2105 (2009).
[48] Daniel B Work, Sébastien Blandin, Olli-Pekka Tossavainen, Benedetto Piccoli, and Alexandre M Bayen. 2010. A traffic model for velocity data assimilation. *Applied Mathematics Research eXpress* 2010, 1 (2010).
[49] Jie Xu, Dingxiong Deng, Ugur Demiryurek, Cyrus Shahabi, and Mihaela van der Schaar. 2015. Mining the situation: Spatiotemporal traffic prediction with big data. *IEEE Journal of STSP* 9, 4 (2015).
[50] Mengwen Xu, Dong Wang, and Jian Li. 2016. DESTPRE: a data-driven approach to destination prediction for taxi rides. In *Proc. of UBICOMP*.
[51] Li Yan and Haiying Shen. 2016. TOP: Vehicle trajectory based driving speed optimization strategy for travel time minimization and road congestion avoidance. In *Proc. of MASS*.
[52] Li Yan, Haiying Shen, Juanjuan Zhao, Chengzhong Xu, Feng Luo, and Chenxi Qiu. 2017. CatCharger: Deploying Wireless Charging Lanes in a Metropolitan Road Network through Categorization and Clustering of Vehicle Traffic. In *Proc. of INFOCOM*.
[53] Jing Yuan, Yu Zheng, Xing Xie, and Guangzhong Sun. 2011. Driving with knowledge from the physical world. In *Proc. of KDD*.
[54] Desheng Zhang, Juanjuan Zhao, Fan Zhang, Ruobing Jiang, and Tian He. 2015. Feeder: supporting last-mile transit with extreme-scale urban infrastructure data. In *Proc. of IPSN*.

[55] Fuzheng Zhang, David Wilkie, Yu Zheng, and Xing Xie. 2013. Sensing the pulse of urban refueling behavior. In *Proc. of UBICOMP*.
[56] Rick Zhang, Federico Rossi, and Marco Pavone. 2016. Routing autonomous vehicles in congested transportation networks: Structural properties and coordination algorithms. *arXiv preprint arXiv:1603.00939* (2016).
[57] Yu Zheng, Tong Liu, Yilun Wang, Yanmin Zhu, Yanchi Liu, and Eric Chang. 2014. Diagnosing New York city's noises with ubiquitous data. In *Proc. of UBICOMP*.
[58] Yu Zheng, Yanchi Liu, Jing Yuan, and Xing Xie. 2011. Urban computing with taxicabs. In *Proc. of UBICOMP*.
[59] Brian D Ziebart, Andrew L Maas, Anind K Dey, and J Andrew Bagnell. 2008. Navigate like a cabbie: Probabilistic reasoning from observed context-aware behavior. In *Proc. of UBICOMP*.

Received May 2017; revised August 2017; accepted October 2017